

# The Two Cultures for Prevalence Mapping: Small Area Estimation and Spatial Statistics

Geir-Arne Fuglstad ([geir-arne.fuglstad@ntnu.no](mailto:geir-arne.fuglstad@ntnu.no))

*Department of Mathematical Sciences, Norwegian University of Science and Technology, Norway*

Zehang Richard Li

*Department of Statistics, University of California Santa Cruz, USA*

Jon Wakefield

*Department of Statistics and Department of Biostatistics, University of Washington, USA*

**Abstract.** The emerging need for subnational estimation of demographic and health indicators in low- and middle-income countries (LMICs) is driving a move from design-based methods to spatial and spatio-temporal approaches. The latter are model-based and overcome data sparsity by borrowing strength across space, time and covariates and can, in principle, be leveraged to create yearly fine-scale pixel level maps based on household surveys. However, typical implementations of the model-based approaches do not fully acknowledge the complex survey design, and do not enjoy the theoretical consistency of design-based approaches. We describe how spatial and spatio-temporal methods are currently used for small area estimation in the context of LMICs, highlight the key challenges that need to be overcome, and discuss a new approach, which is methodologically closer in spirit to small area estimation. The main discussion points are demonstrated through two case studies: spatial analysis of vaccination coverage in Nigeria based on the 2018 Demographic and Health Surveys (DHS) survey, and spatio-temporal analysis of neonatal mortality in Malawi based on 2010 and 2015–2016 DHS surveys. We discuss our key findings both generally and with an emphasis on the implications for popular approaches undertaken by industrial producers of subnational prevalence estimates.

**Keywords:** Bayesian smoothing; complex survey designs; demographic and health indicators; design-based inference; geostatistical models; validation.

## 1. Introduction

Accurate tracking of the Sustainable Development Goals (SDGs) set forth in General Assembly of the United Nations (2015) requires the estimation of a range of demographic and health indicators across all countries of the world. We focus on indicators that can be expressed as proportions of individuals that are in the binary states of interest. Examples include neonatal mortality rate (NMR), vaccination coverage, female attainment of specific years of education, and proportions of children who are classified as low birth weight. In addition to monitoring attainment of targets, subnational estimates of such indicators are a key aid to constructing effective health policies and ensuring that no one

is left behind in implementing the United Nations 2030 development agenda (UN System Chief Executives Board for Coordination, 2017).

The subnational areas of interest are the first administrative level (admin1) and the second administrative level (admin2), which are nested partitions of the national level (admin0) geography. Admin2 is the level at which many health policy decisions are made (Hosseinpoor et al., 2016). In many low- and middle-income countries (LMICs), a reliable data source is provided by household surveys such as the Demographic and Health Surveys (DHS)<sup>†</sup> and the Multiple Indicator Cluster Surveys (MICS)<sup>‡</sup>. Both conduct stratified two-stage cluster sampling. A country is first divided into geographical strata that are crossed with an urban/rural indicator, and then further into small enumeration areas (EAs), also called clusters, consisting of collections of households. A survey is conducted by sampling a specific number of clusters in each stratum, and sampling a specific number of households within each selected cluster. This means that each household has an inclusion probability that describes the *a priori* probability that it will be included in the sample. Recent survey samples are point-referenced, and there are two main strategies for subnational mapping: design-based small area estimation (SAE) approaches and spatial/spatio-temporal statistical approaches. The former is explicitly linked to the data collection process and directly considers the discrete areas of interest, and the latter usually pays scant attention to the survey design and treats space continuously.

DHS surveys are typically powered to admin1, i.e., they contain sufficient samples for reliable estimation of key indicators for admin1 areas. Hence, at admin1, it is natural to report survey estimates, which use information on the survey design and the inclusion probabilities through weighted estimators. In the language of SAE (Rao and Molina, 2015), a weighted estimate is an example of a *direct estimate* that only uses information on the response variable for the specific area. By contrast, *indirect estimates* allow borrowing of response information from other areas. The seminal Fay and Herriot (1979) model provides an early example of a hierarchical indirect area-level model, in which a (transformed) weighted estimate is taken as response. Many extensions of the Fay-Herriot model, including the use of discrete spatial models and area-level covariates, have been proposed (You and Zhou, 2011; Marhuenda et al., 2013; Mercer et al., 2015; Watjou et al., 2017). These SAE models are called *area-level models* because aggregated response variables are modeled. A key feature is that the survey design is acknowledged through the use of weighted estimators and their associated variances.

A more flexible SAE approach is provided by *unit-level models* that are specified at the level of the cluster and include area-level random effects (Battese et al., 1988). The challenges with unit-level models are that: (i) they require model terms that explicitly acknowledge the design, and (ii) area-level estimates are not directly available without an aggregation procedure. With respect to (i), fixed effects are typically included to account for stratification, and independent random effects are included to account for the clustering aspect. In many settings, it is common practice to include covariates at either the area- or the unit-level. However, as regards (ii), in the context of LMICs, including cluster- or individual-specific covariates is challenging since aggregation to produce area-

<sup>†</sup><https://dhsprogram.com/>

<sup>‡</sup><https://mics.unicef.org/>

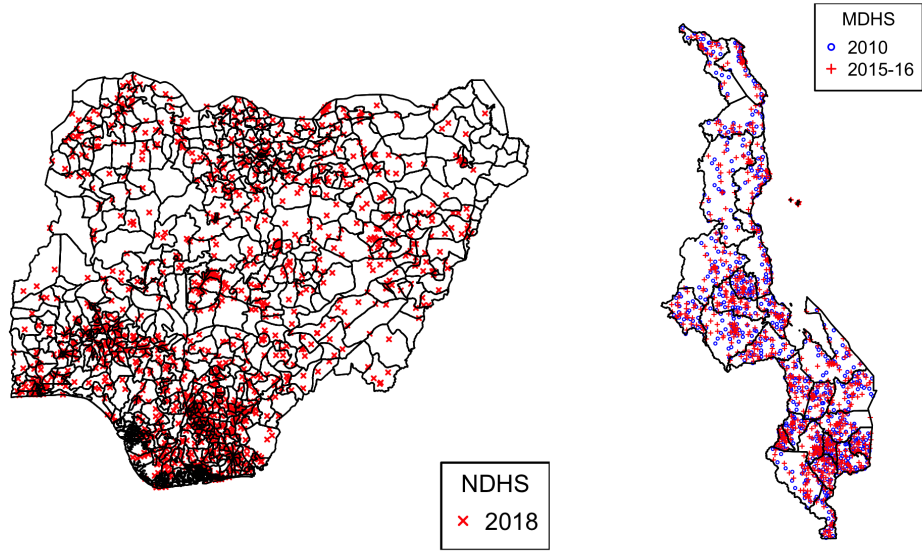
level estimates requires reliable covariate values for the unobserved units, and these are not usually available. More details and further variations of area-level and unit-level SAE models can be found in Rao and Molina (2015).

When the surveys are not powered to the desired subnational level, design-based approaches break down since target areas may have few or no sampled units. However, unit-level spatial models that includes variation over continuous space, i.e., geostatistical models, can still produce pixel maps (e.g., at the  $1 \times 1$  km or  $5 \times 5$  km level) for a range of indicators (Diggle and Giorgi, 2016; Golding et al., 2017; Utazi et al., 2020; Local Burden of Disease Vaccine Coverage Collaborators and others, 2021). To facilitate the comparison of such methods with SAE approaches, we make a distinction between *prevalence*, which is the empirical proportion of the finite population within the administrative area who are in the binary state, and *risk*, which is the analogous proportion of a hypothetical infinite population. SAE approaches perform *prevalence mapping*, i.e., the empirical proportions for areas are estimated and mapped, while most current endeavors using spatial statistics approaches approximate prevalences through *risk mapping*, where areal risk estimates are extracted based on a geostatistical model.

More specifically, a geostatistical model is expressed in terms of an unobservable spatial or spatio-temporal risk surface that exists independently of the finite population. Each point-referenced observation is viewed as the result of a group of individuals being exposed to the risk at the given location. The risk surfaces are described in terms of Gaussian random fields and spatio-temporal covariates, and may borrow strength across space, time and covariates. Geostatistical models work even in extremely data sparse settings, but two major challenges with such approaches are to convert estimated risk surfaces to prevalence estimates for administrative areas (Dong and Wakefield, 2021; Paige et al., 2021) and to acknowledge complex survey designs (Paige et al., 2020).

For linear models, both the SAE and the spatial statistics literature are interested in optimal linear predictors. The former in the context of finite population summaries such as means and totals, and the latter in terms of point predictions or averages over areas. However, for binary outcomes, since the observation model is non-linear and auxiliary population information is needed for aggregation, it is not obvious that optimal predictions at a given spatial resolution, say pixel-level or admin2, will translate to optimal predictions at coarser levels such as admin1 or admin0. In this paper, we formally evaluate the accuracy and precision of different approaches with the aim being to provide a recommended workflow for prevalence mapping.

We describe a model-based approach for subnational estimation with a discrete spatial model in which the risk surface is constant at the specified administrative level at which inference is required. Our approach acknowledges key parts of the survey design such as stratification and clustering, but does not directly acknowledge the inclusion probabilities. Through the case studies, we emphasize that estimation at different administrative levels may call for different approaches. The first case study is spatial estimation of vaccination coverage for admin1 and admin2 areas in Nigeria in 2018. We compare the new approach, standard geostatistical models, and design-based approaches through quantitative model validation based on cross-validation of cluster-level predictions and hold-out-area validation of admin1 estimates. The second case study is spatio-temporal estimation of yearly NMRs for admin2 areas in Malawi and for this example we inves-



(a) 774 local government areas in Nigeria.

(b) 28 districts in Malawi.

**Figure 1.** Admin2 areas for (a) Nigeria and (b) Malawi. The points show the sampled clusters in the surveys. Information about the surveys are found in Table 1.

**Table 1.** Summary of the surveys. R is rural and U is urban. The sampling frame for NDHS2018 is based on the 2006 census, but the frame was updated in 2017.

Country	Survey	Census	Strata	R clusters	U clusters
Malawi	MDHS2010	2008	54	691	158
Malawi	MDHS2015-16	2008	56	677	173
Nigeria	NDHS2018	2006(2017)	74	820	580

tigate the importance of different model choices for producing predictions of NMR. The admin2 areas for Nigeria and Malawi are shown in Figure 1 and the DHS surveys used are listed in Table 1. For Nigeria we also consider the coarser admin1 areas as seen in Figure 3.

In the remainder of the paper, we first detail the data sources and motivate the two case studies in Section 2. Then we describe and discuss the core ideas of design-based inference and spatial smoothing of design-based estimates in Section 3. This is followed by a detailed discussion on the model-based approach, hierarchical spatial and spatio-temporal models, and spatial aggregation in Section 4. We present the most important results from the case studies in Section 5, and the paper ends with discussion in Section 6. Model details and additional results are relegated to the appendicies, and data and code are available at <https://github.com/gafuglstad/prevalence-mapping>.



## 2. Motivation

### 2.1. *Spatial estimation of vaccination coverage in Nigeria*

Extensive efforts to map vaccination coverage has lead to the production of many detailed maps including for the measles vaccine (Takahashi et al., 2017) and for the diphteria-pertussis-tetanus vaccine (Mosser et al., 2019). High-resolution maps are being created through geostatistical models (Utazi et al., 2018a,b), and may have the potential to guide vaccination programs (Utazi et al., 2019). However, Dong and Wakefield (2021) highlight the need for visualization techniques that account for the considerable uncertainty in such maps when they are used to identify areas of low and high vaccination coverage.

We consider vaccination coverage for the first dose of measles-containing-vaccine (MCV1) among children aged 12–23 months in Nigeria. The goal of the analysis is estimation of MCV1 coverage for admin1, which consists of 36 states and the federal capital area, and admin2, which consists of 774 local government areas (LGAs), and to this end we analyze the 2018 Nigeria Demographic and Health Survey (NDHS2018; National Population Commission - NPC and ICF (2019)). For children in the sampled households, vaccination status is decided from either vaccination cards or caregiver recall. Area-level approaches are applicable for admin1 areas, but not for admin2 areas due to data sparsity. Unit-level models, where the units are the EAs, are applicable both for admin1 and admin2 areas. The data is collected under a complex survey design, and the key question is which approaches result in reliable estimates. The key finding is that one should model at the administrative level at which prevalences are desired.

The sampling frame is based on the 2006 census and divides Nigeria into 664,999 census EAs. The urban/rural classification of the EAs was updated in 2017; for details see National Population Commission - NPC and ICF (2019, Appendix A.2). Nigeria was stratified into 74 strata: 37 admin1 areas crossed with urban and rural. Within each stratum a two-stage clustered sampled was drawn; see Section 3.2 for a general description. There are 1389 clusters for which data were successfully collected; data could not be obtained for a number of the clusters that were on the list to be sampled, because of law and order concerns. For Borno this was particularly problematic, and the estimates for this state should be interpreted with caution, see National Population Commission - NPC and ICF (2019) for further details. The admin1 areas are explicitly known and though the admin2 areas are not known, we can derive this information for most clusters, since 1382 clusters have GPS coordinates.

### 2.2. *Spatio-temporal estimation of NMR in Malawi*

NMR is the proportion of deaths during the first 28 days for live births, and is a key indicator in SDG 3.2 with a specific target of less than 12 deaths per 1000 live births for every country, by 2030. Recent efforts have provided detailed high-resolution maps of NMR and other child mortality indicators for LMICs using geostatistical models (Golding et al., 2017; Burstein et al., 2019).

We consider spatio-temporal estimation of NMR in Malawi. The goals are yearly estimates of NMR for admin2, which consists of 28 districts, for the years 2000–2016, and short term predictions for 2017–2019. We use the 2010 (MDHS2010; National Statistical Office - NSO/Malawi and ICF Macro (2011)) and 2015–2016 (MDHS2015-16;

National Statistical Office/Malawi and ICF (2017)) DHS surveys. In each visited household, women aged 15–49 that spent the night before in the household were asked to list all live births including dates of birth for all children and dates of death for children who have died. This is termed full birth history data, and each survey provides retrospective information from the time of the survey. Area-level approaches cannot produce reliable estimates due to data sparsity, and we investigate different unit-level approaches with a focus on the importance of model choice in the context of forecasting. The key finding is that forecasts show high sensitivity to model choice.

The sampling frame for each of the MDHS2010 and MDHS2015-16 surveys is based on the 2008 census and divides Malawi into 12,569 EAs, where each EA is classified as urban or rural. The stratification varies between the two surveys, but for each survey, urban and rural is crossed with a set of geographical areas. See Table 1 for information on the number of strata. In each stratum, two-stage clustered sampling was conducted as described in Section 3.2. MDHS2010 has 849 clusters and MDHS2015-16 has 850 clusters, and admin2 areas are known for all clusters.

### 3. Design-based analysis

#### 3.1. Finite populations and target parameters

In design-based inference, we consider a finite target population in a study area that consists of  $N > 0$  *observation units*. In the motivating examples, these units are the children aged 12–23 months at a given point in time and the live births that occurred in a given time period, respectively. The target population can be represented as the set of indices  $U = \{1, 2, \dots, N\}$  where unit  $i$  has an associated value  $y_i \in \{0, 1\}$  for  $i \in U$ . These values are deterministic and unknown. When a country is divided into  $A$  administrative areas, these areas partition the population  $U$  into  $A$  disjoint subpopulations,  $U = U_1 \cup U_2 \cup \dots \cup U_A$ , where  $U_a$  is the set of units that belong to area  $a$ .

Let  $N_a$  denote the number of units in  $U_a$ , then the target parameters are the area-specific prevalences  $p_a = \sum_{i \in U_a} y_i / N_a$ ,  $a = 1, 2, \dots, A$ . If the units consist of observations over different time periods, we let  $U^{(t)}$ ,  $t = 1, 2, \dots, T$ , denote the target population at time period  $t$  and let  $U_a^{(t)}$  denote the population in area  $a$  at time  $t$ . If  $N_a^{(t)}$  denotes the number of units in  $U_a^{(t)}$ , then the target prevalences are

$$p_{a,t} = \frac{1}{N_a^{(t)}} \sum_{i \in U_a^{(t)}} y_i, \quad a = 1, 2, \dots, A, \quad t = 1, 2, \dots, T. \quad (1)$$

#### 3.2. Complex survey samples

Censuses are conducted in LMICs at best every tenth year and from each census a *master sampling frame*, which aims to be an enumeration of the households, is constructed. Each master sampling frame assigns every household in the census to an EA. The EAs are classified as urban/rural by national authorities at the time of the census (based on their own definition), and in some cases, such as NDHS2018, the classifications are updated between the time of the census and the survey.

DHS conducts *household surveys*, approximately every fifth year, where the sampled units are households, selected based on the latest master sampling frame. DHS surveys are generally conducted with a stratified two-stage cluster sampling design, as detailed in ICF International (2012). The country is stratified by a set of geographic areas, often admin1, crossed with urban/rural. In the survey, pre-specified numbers of urban EAs and rural EAs are sampled in each area. In the first stage, EAs are sampled from strata with selection probabilities proportional-to-size (with size corresponding to number of households). The sampled EAs are termed primary sampling units (PSUs) or *clusters*. Since the lists of households in the master sampling frame are likely to be outdated, an up-to-date list of households is collected for each cluster. Then in the second stage, the same fixed number (often between 20 and 35) of households are sampled with equal probability from the updated list of households in each cluster. The households are termed secondary sampling units (SSUs).

The result of this process is a random subset  $S_H$  of all households in the master sampling frame, where household  $h$  has an *inclusion probability*  $\pi_h = P(h \in S_H)$ . These probabilities are constructed from the probabilities of stratum selection and the probabilities of sampling from the two subsequent levels of clustering. Survey weights are defined as  $w_h = 1/\pi_h$ . A non-response adjustment is usually made by scaling the weights. The total number of households in each EA is not available, and the constituent parts of the final weights are not released. The weights are also scaled, with the scaling factor not released, so totals cannot be easily estimated, though proportions can.

Information on specific target populations is secured via interviews from members of the households. Thus the data collected by a household survey can also be viewed as a random sample of units from the target populations discussed in Section 3.1. Similarly, for events in the past, we may construct retrospective units in random subsets  $S_a^{(t)} \subset U_a^{(t)}$  for  $a = 1, 2, \dots, A$  and  $t = 1, 2, \dots, T$ . Critically, the inclusion probability of each unit equals that of the household. Let  $h[i]$  and  $a[i]$  denote the household and area from which unit  $i$  was extracted, respectively. Then the inclusion probability of unit  $i$  is  $P(i \in S_{a[i]}^{(t)}) = P(h[i] \in S_H)$ . For the remainder of the paper, the index  $i$  denotes the units of the target population.

Importantly, the geographic stratification on area crossed by urbanicity can vary between surveys due to several reasons. The administrative regions may be redrawn and newer surveys may be powered to a finer administrative level. Furthermore, the urbanicity status of an EA may change over time because of the redrawing. But, when model-based procedures adjust for the urban/rural stratification, the recorded stratification variable should be viewed as a *fixed partition* over time, because it is not the *current* urban/rural state of the cluster, but rather the state at the time the sampling frame was constructed. In Section 6, we briefly discuss the added difficulty arising from differing definitions of urban and rural EAs for different sampling frames.

### 3.3. Direct estimates

For a single survey, the weighted estimator (Horvitz and Thompson, 1952; Hájek, 1971) replaces the numerator and denominator in Equation (1) with the survey weighted esti-

mates, i.e.,

$$\hat{p}_{a,t}^{\text{HT}} = \frac{\sum_{i \in S_a^{(t)}} w_i y_i}{\sum_{i \in S_a^{(t)}} w_i}, \quad a = 1, 2, \dots, A, \quad t = 1, 2, \dots, T. \quad (2)$$

Stochasticity arises from repeated sampling under the complex survey design, and the random quantity in the above equation is  $S_a^{(t)}$ . The estimators of the numerator and the denominator are unbiased, and  $\hat{p}_{a,t}^{\text{HT}}$  is approximately unbiased for  $p_{a,t}$ . Design-based estimates of variance can be made with the linearized or jackknife estimator (Lohr, 2009), and the R package `survey` (Lumley, 2004) provides an implementation for generalized linear models.

When there are  $K$  surveys, direct estimates  $\hat{p}_{a,t,k}^{\text{HT}}$  can be calculated for each survey separately. Reliable estimates with low variances require sufficient sample sizes for each combination of  $a$ ,  $t$  and  $k$  values. However, the  $A$  administrative areas may be unplanned areas (Lehtonen and Veijanen, 2009), which do not match the stratification, so that some administrative areas have few clusters. More generally, the sample sizes of DHS surveys are too low to make reliable yearly estimates at admin2.

### 3.4. Leveraging spatio-temporal dependence

Direct estimates can be viewed as observations of the true area-specific prevalences. This was the rationale behind the celebrated Fay and Herriot (1979) model where the design information was implicitly contained through the use of the weighted estimate and its standard error. These areal estimates were smoothed with the estimate possibly transformed to improve the asymptotic approximation to the sampling distribution. We describe in more detail in the context of a prevalence. We have a Gaussian approximation for survey  $k = 1, 2, \dots, K$ ,

$$h_{a,t,k} | \eta_{a,t,k}, \hat{V}_{a,t,k} \sim \mathcal{N}(\eta_{a,t,k}, \hat{V}_{a,t,k}), \quad a = 1, 2, \dots, A, \quad t = 1, 2, \dots, T,$$

where  $h_{a,t,k} = \text{logit}(\hat{p}_{a,t,k}^{\text{HT}})$  is the estimated logit-prevalence,  $\eta_{a,t,k} = \text{logit}(p_{a,t,k})$  is the true logit-prevalence after accounting for survey-specific non-sampling errors, and  $\hat{V}_{a,t,k}$  is a design-based estimate of the variance of  $\text{logit}(\hat{p}_{a,t,k}^{\text{HT}})$ . This formulation provides the potential to reduce the uncertainty in the estimated prevalences by borrowing strength across space, time, and covariates.

Mercer et al. (2015) proposes an extension of the ideas of the Fay-Herriot model where they employ a spatio-temporal latent model. A simple (covariate-free) latent model is to assume that regions  $a = 1, 2, \dots, A$  for times  $t = 1, 2, \dots, T$  satisfy

$$\begin{aligned} \eta_{a,t,k} &= \alpha_{a,t} + \nu_k + \text{BIAS}_{a,t} \\ &= (\mu + e_a + v_a + b_t + \delta_{a,t}) + \nu_k + \text{BIAS}_{a,t}, \quad k = 1, 2, \dots, K, \end{aligned}$$

where  $\alpha_{a,t} = \text{logit}(p_{a,t})$  is the true logit-prevalence and is composed of an intercept  $\mu$ , a structured random effect  $(e_1, \dots, e_A)$  such as Besag's ICAR model (Besag et al., 1991), an unstructured random effect  $(v_1, \dots, v_A)$ , a temporal random effect  $(b_1, \dots, b_T)$  such as a second-order random walk (RW2), and a random effect describing the spatio-temporal interaction,  $(\delta_{1,1}, \dots, \delta_{A,T})$ . Further  $(\nu_1, \dots, \nu_K)$  is an unstructured effect describing

survey errors, and  $\text{BIAS}_{a,t}$  describes systematic biases across surveys for area  $a$  at time  $t$ . More details about the model components can be found in Mercer et al. (2015) and Li et al. (2019). The systematic bias correction is discussed for the effect of maternal mortality caused by HIV on the estimation of under-5 mortality in Wakefield et al. (2019) and Li et al. (2019). In the context of NMR, corrections are more challenging as the extra maternal mortality caused by HIV will bias the observations, but AIDS related deaths are uncommon in the neonatal time period (Alexander and Alkema, 2018).

We will term estimates produced by the above procedure as *smoothed direct* estimates. We emphasize that it is the prevalence that is being modeled, and not the risk. The above procedure assumes that the direct estimates arise independently of each other. If this condition fails, spatial or temporal autocorrelation in the direct estimates may be picked up by the latent model. In space this assumption is expected to be fulfilled. In time the same clusters will contribute to all time points, but the use of several surveys may compensate for this.

For SAE, a large emphasis is placed on estimating the mean squared error (MSE) associated with an areal estimate, with the bootstrap being a popular tool. A good discussion of design-based and model-based approaches to MSE estimation is provided by Datta et al. (2011). Under a fully Bayesian approach, as discussed in Section 4, the natural analog is the posterior variance, which is a model-based estimate.

### 3.5. Advantages and disadvantages

The major advantage of design-based approaches is that they account for the sampling design and achieve design consistency, in the sense that the (design) bias and variance of the estimated prevalence tend to zero as one considers a sequence of growing finite populations, along with a sequence of sampling designs with the ratio of the sample size to the population size converging to a fixed constant; for a good overview see Breidt and Opsomer (2017). The major drawbacks are the practical and financial difficulties in collecting a large enough sample to be able to use the approach for SAE in the context of granular spatio-temporal resolution. For example., there are 774 LGAs in Nigeria, but only 1389 clusters in NDHS2018, and for NMR there are many combinations of areas and years where no births are sampled. If high quality auxiliary data is available for all the population, model-assisted methods (Lehtonen and Veijanen, 2009) could leverage the auxiliary information while maintaining design-consistency. However, in the context of LMICs, demographic data of such a type are typically unavailable. These difficulties motivate the need to look beyond the traditional design-based methods and consider model-based methods that are prolific in the analysis of spatio-temporal data in other contexts (Cressie and Wikle, 2011).

## 4. Model-based analysis

### 4.1. A model-based perspective

We focus on the spatial setting to simplify the presentation and the notation. Consider the finite target population in Section 3.1 to be a draw from a hypothetical superpopulation. Then the outcome  $y_i$  of unit  $i$  is a realization of a stochastic variable  $Y_i$  for  $i = 1, \dots, N$ , and the target prevalence  $p_a$  in the finite population is a realization of the

stochastic variable  $P_a = \sum_{i \in U_a} Y_i / N_a$  for  $a = 1, \dots, A$ , where  $N$  and  $U$  are fixed. A survey sample consists of two parts: the sampled random subset  $S = s \subset U$  and the associated outcomes  $\mathbf{y}_s = (y_i)_{i \in s}$ , which is a realization of the random vector  $\mathbf{Y}_S = (Y_i)_{i \in S}$  when  $S = s$ .

For area  $a$ , we can decompose the prevalence as

$$P_a = \frac{1}{N_a} \left( \sum_{i \in S_a} Y_i + \sum_{i \in U_a \setminus S_a} Y_i \right),$$

where the first and second terms consist of observed and unobserved units, respectively. After sampling, the first term is known, and the estimation of  $p_a$  essentially requires prediction of the second term. To this end, one specifies a unit-level model for outcomes,  $Y_i$ , that depend on auxiliary information such as spatial locations and covariates, estimates the model based on the survey sample, and predicts the unobserved outcomes. We return to the issue of how this aggregation from unit-level to area-level can be performed for spatio-temporal models in Section 4.4.

If the units are selected using a complex survey design and this is not accounted for explicitly in the unit-level model, the resulting estimates  $p_a$  can be biased or have misleading uncertainty estimates. A simple example is when the sampling design oversamples urban units relative to rural units, but the model does not separate between urban and rural units. Then if the prevalence among urban units is higher than the prevalence among rural units, one would expect to overestimate the prevalence  $p_a$ . Generally, the posterior of  $P_{a,t} | \mathbf{Y}_S = \mathbf{y}_S, S = s$  is only equal to the posterior of  $P_{a,t} | \mathbf{Y}_s = \mathbf{y}_s$  if we specify a model for the outcomes that results in the complex survey design being ignorable (Sugden and Smith, 1984).

Here we focus on two main components in the design of DHS surveys that makes  $S = s$  informative: stratification and clustering. In a stratified sample, some strata tend to be oversampled compared to other strata, and using a model where strata share model parameters and model components (so that strata are indistinguishable) may lead to biased estimates. A simple way to make stratification ignorable is to fit separate models in each stratum (Little, 2003), but then the models cannot borrow strength across strata. In a clustered sample, we sample clusters of units and if the outcomes in the clusters are correlated, the effective sample size is smaller than the apparent sample size (Gelman and Hill, 2006). The consequence is that the estimated variances of the model components will tend to be too small. When the aim is to achieve ignorability of the complex survey design, one needs to consider and to acknowledge the design in the model specification (Sugden and Smith, 1984; Pfeffermann, 1993).

We wish to carefully evaluate the recent trend of using geostatistical methods for producing fine-scale pixel maps and prevalence estimates (Diggle and Giorgi, 2019; Burstein et al., 2019; Utazi et al., 2020). It is becoming common to include an unstructured cluster-specific random effect to account for the dependence between units sampled in the same cluster (Scott and Smith, 1969), but it is not commonplace to explicitly acknowledge the stratification by urban and rural. Paige et al. (2020) demonstrate that not accounting for the stratification by urban and rural can lead to bias. Spatial and spatio-temporal methods open new possibilities over design-based approaches in data

sparse situations, but we need to understand how much of the design we need to acknowledge to produce reliable small area estimates. We leave the discussion of the role of PPS sampling, adjustments for nonresponse, jittering of GPS coordinates, raking and poststratification to Section 6.

## 4.2. Cluster-level modelling

### 4.2.1. Notation

We group units in the same cluster and consider cluster-level models. We index observed outcomes by cluster  $c = 1, \dots, M_k$  at time  $t = 1, \dots, T$  in survey  $k = 1, \dots, K$ , and let  $n_{c,t,k}$  be the sampled number of individuals at risk and  $y_{c,t,k}$  be the subsequent number of events. For cluster  $c$  in survey  $k$ , we assume that we know the geographical coordinates,  $\mathbf{s}_{c,k} \in \mathbb{R}^2$ , and the urbanicity,  $\text{Urb}[c, k] \in \{\text{U}, \text{R}\}$ . Cluster-level covariates  $\mathbf{z}_{c,t,k}$  may vary both between clusters and across time. We do not include household-specific covariates or random effects because the number of trials in households are typically low and we lack reliable household-level information for the population (which is needed for aggregation). For spatial modelling such as vaccination coverage in Section 5.1, we drop the time index.

### 4.2.2. Modelling without urban and rural stratification

Recall that risk is a hypothetical, infinite population quantity, whereas prevalence is an empirical, finite population quantity. We present prevalence mapping in two steps: we express the cluster-level models in terms of risk in Sections 4.2 and 4.3, and then we discuss how to extract areal prevalence maps in Section 4.4. We assign risks  $r_{c,t,k}$  to clusters  $c = 1, \dots, M_k$  at times  $t = 1, \dots, T$  in surveys  $k = 1, \dots, K$ . By our definition of risk, the expectation of the prevalences for the sampled units in the sampled clusters should match the risks, i.e.,  $E[Y_{c,t,k}/n_{c,t,k} | r_{c,t,k}] = r_{c,t,k}$ . However, we do not expect the sampling distribution of  $Y_{c,t,k} | n_{c,t,k}, r_{c,t,k}$  to be binomial due to overdispersion arising from sampling households within the clusters instead of simple random sampling of units. We will not consider misclassification error models. We follow Dong and Wakefield (2021) and consider two options for overdispersed binomial distributions:

1. **Beta-Binomial:**  $Y_{c,t,k} | n_{c,t,k}, r_{c,t,k}, d \sim \text{Beta-Binomial}(n_{c,t,k}, r_{c,t,k}, d)$ , where the notation  $Y | n, r, d \sim \text{Beta-Binomial}(n, r, d)$  indicates the beta-binomial distribution with  $E[Y/n | n, r, d] = r$  and  $\text{Var}[Y/n | n, r, d] = r(1-r)(1 + (n-1)d)/n$ .
2. **Lono-Binomial:**  $Y_{c,t,k} | n_{c,t,k}, R_{c,t,k}^A \sim \text{Binomial}(n_{c,t,k}, R_{c,t,k}^A)$ , where the logit of the apparent risk,  $\text{logit}(R_{c,t,k}^A) = \text{logit}(R_{c,t,k}) + \epsilon_{c,t,k}$ , is a combination of a baseline logit risk, and independent and identically distributed  $\epsilon_{c,t,k}$  according to  $\mathcal{N}(0, \sigma_N^2)$ . The **Lono-** part of the label highlights the assumed lognormal distribution contribution to the risk odds.

Since each cluster is sampled once, it is impossible to separate overdispersion due to the sampling design and true unstructured between-cluster variation. This is particularly clear for the Lono-Binomial where the unstructured cluster effects could also be interpreted as true variation. Under the assumption of overdispersion,  $r_{c,t,k} \neq R_{c,t,k}$  and one needs to average over the distribution of  $\epsilon$  to find  $r_{c,t,k}$ ; it is straightforward to do this,

though it adds computational burden, and so instead we focus on Beta-Binomial models. In practice, we have found little substantive differences between Beta-Binomial and Lono-Binomial models. In Section 4.4, we discuss why the interpretation of the cluster effects matters for spatial aggregation, and in Section 5.1, we demonstrate the practical difference through Lono-Binomial for estimation of vaccination coverage in Nigeria.

The latent spatio-temporal variation in logit risk is described as

$$\begin{aligned} \text{logit}(r_{c,t,k}) = & \mu + \text{Covariates}(c, t, k) + \text{Survey}(k) \\ & + \text{Time}(t) + \text{Space}(\mathbf{s}_{c,k}) + \text{Space-Time}(\mathbf{s}_{c,k}, t), \end{aligned} \quad (3)$$

where  $\mu$  is the intercept. For the Lono-Binomial choice, we would model  $\text{logit}(R_{c,t,k})$ . The strong confounding between the intercept, the main temporal effect, the main spatial effect, and the spatio-temporal interaction necessitates the use of constraints to make the model identifiable (Knorr-Held, 2000). We provide a thorough description of commonly used model components and constraints in Appendix A. In Section 4.3, we use the above framework to propose a new approach and discuss currently used geostatistical approaches.

#### 4.2.3. *Modelling with urban and rural stratification*

As discussed in Section 4.1, we should acknowledge the stratification by urbanicity in the survey design by stratifying the model by urbanicity. However, stratifying the latent model in Equation (3) by urban and rural hinges on sufficient power in the data to estimate stratum-specific effects, and one needs to strike a balance between complexity and feasibility. E.g., we may choose to not stratify the spatial and spatio-temporal interaction, but to stratify the main temporal effect with respect to urban/rural. We discuss the challenges that arise in spatial prediction in Section 4.4.

#### 4.2.4. *Recent approaches for vaccination coverage and NMR estimation*

MCV1 vaccination coverages have been estimated for  $5 \text{ km} \times 5 \text{ km}$  pixels, admin2 areas and admin1 areas in 101 LMICs by Local Burden of Disease Vaccine Coverage Collaborators and others (2021). They follow a three step approach: 1) selecting covariates, 2) fitting a geostatistical model with a Matérn Gaussian random field (GRF) for the spatial structure and an AR(1) process for the temporal structure, and 3) calibrating to global burden of disease model estimates. In the geostatistical model, the binomial likelihood in Section 4.2.2 is used with separate nugget effects for each pixel and year combination. The models are fitted across several countries jointly and use many data sources.

This approach is similar to the approach used in Burstein et al. (2019) and Golding et al. (2017) for NMR and under-five mortality rate (U5MR). The major difference is that the child mortality models must allow for separate mortality in different age bands since the immediate risk of death varies by the age of the child. The details of such models are beyond the scope of this paper, but a joint approach for NMR and U5MR allows estimates of NMR that borrow strength from later age bands (Wakefield et al., 2019).



In addition to MCV1, coverage of diphtheria-tetanus-pertussis-containing vaccine have been considered. Early models were formulated with a standard binomial likelihood with no overdispersion (Utazi et al., 2018a, 2019), but later work has included nuggets associated with each cluster (Utazi et al., 2020). The latter employ cluster-level geostatistical models incorporating covariates and a spatial Matérn GRF. Empirical evidence on the treatment of the nugget in aggregation is mixed: results in Utazi et al. (2021) indicate that the nugget is not important after aggregating to admin1 estimates, while Dong and Wakefield (2021) find that the treatment of the nugget effect can affect the estimates.

While there has been a push towards fine-scale modelling, the DHS report for surveys such as NDHS2018 (National Population Commission - NPC and ICF, 2019) use direct estimates for vaccination coverage and NMR, while the smoothed direct approach in Section 3.4 has been used for child mortality (Mercer et al., 2015; Li et al., 2019). The focus was U5MR, but the method also produced estimates of NMR.

In the next section we describe models that we have found useful in a LMICs context. The linear predictor of the model can be used with either the Lono-Binomial likelihood or the beta-binomial likelihoods described in Section 4.2.2. We use the former for vaccination coverage in Section 5.1 and the latter for NMR in Section 5.2. Lono-Binomial models allow us more freedom in exploring the cluster effects, but Beta-Binomial models are computationally faster.

### 4.3. The Beta-Binomial model

We propose a geostatistical model with a piece-wise constant spatial effect, so that we have a discrete spatial model. For reasons we will elaborate upon, we recommend picking the spatial resolution to match the administrative level at which estimates are desired. A more complex version of this approach was recently applied to produce subnational U5MR estimates for 22 LMICs (UN IGME, 2021) in close coordination with the United Nations Inter-agency Group for Mortality Estimation (UN IGME). Initial estimates were shared through country consultation and we subsequently addressed the respective countries concerns. The estimates are reproducible using the R package SUMMER (Li et al., 2021, 2020), which implements the approach.

The Beta-Binomial model is specified through the beta-binomial likelihood and the latent model specification in Equation (3). We rescale intrinsic (improper) model components as described in Sørbye and Rue (2014), and suggest the use of PC priors for the parameters (Simpson et al., 2017; Sørbye and Rue, 2017; Riebler et al., 2016). UN IGME (2021) and Wu et al. (2021) illustrate that this class of priors work well with the default hyperparameters in SUMMER across diverse countries for spatio-temporal estimation, but results should always be carefully scrutinized for anomalous behavior. See the appendices for specific choices of hyperparameters in the context of the case studies. In this section, we describe the key information for each of the model components, and  $\mathcal{N}(0, \mathbf{Q}^{-1})$  should be understood as the intrinsic model with precision matrix  $\mathbf{Q}$  when  $\mathbf{Q}$  is singular.

*Survey effects and covariates*

There may be systematic differences between surveys, and we allow the risk to be shifted between surveys through fixed effects,  $\text{Survey}(k) = \nu_k$ , where  $\nu_1, \dots, \nu_K \stackrel{\text{iid}}{\sim} \mathcal{N}(0, 1000)$ . We apply a sum-to-zero constraint on the  $\nu_k$ 's. If there is only one survey, this model component is not included. We fix the variance in the prior because the number of surveys will be small. In Li et al. (2020) and UN IGME (2021), no covariates were used, but covariates available over space-time are easily accommodated through

$$\text{Covariates}(c, t, k) = \mathbf{z}(\mathbf{s}_{c,k}, t)\boldsymbol{\beta},$$

where  $\mathbf{z}(\cdot, \cdot)$  is a  $p$ -variate vector of covariates, and  $\boldsymbol{\beta} \sim \mathcal{N}_p(\mathbf{0}, 1000\mathbf{I})$ . The covariates could either be cluster-specific, admin2-specific, or admin1-specific, but cluster-specific covariates make aggregation challenging.

*Temporal main effect*

We capture temporal changes in overall risk through a main temporal effect. We stratify by urban/rural to acknowledge the stratified sampling design and the potential difference between risk in urban and rural clusters. For cluster  $c$  in survey  $k$ , we let

$$\text{Time}(c, t, k) = \mu_{\text{Urb}[c,k]} + \gamma_{\text{Urb}[c,k],t}, \quad t = 1, \dots, T,$$

where  $\text{Urb}[c,k] \in \{\text{U}, \text{R}\}$ . The two strata are given independent and identical distributions. For stratum U, we choose  $\mu_{\text{U}} \sim \mathcal{N}(0, 1000)$  and  $\boldsymbol{\gamma}_{\text{U}} = (\gamma_{\text{U},1}, \dots, \gamma_{\text{U},T}) \sim \mathcal{N}_T(\mathbf{0}, \mathbf{Q}_{\text{Time}}^{-1})$ . For stratum R, we use the same structure. Examples of temporal models are first-order random walk (RW1), RW2 and autoregressive processes of order 1 (AR(1)). For RW1 and RW2 models, we apply a sum-to-zero constraint,  $\sum_{t=1}^T \gamma_{\text{U},t} = 0$ , to avoid confounding with the intercept  $\mu_{\text{U}}$ . The parameter vector  $\boldsymbol{\theta}_{\text{Time}}$  is either one-dimensional (for RW1 and RW2) or two-dimensional (for AR(1)). We investigate the significance of the choice of temporal model in Section 5.2.

*Main spatial effect*

We choose a continuously indexed spatial effect based on an areal model,

$$\text{Space}(\mathbf{s}_{c,k}) = \sigma_{\text{Space}} \left( \phi_{\text{Space}} v_{a[\mathbf{s}_{c,k}]} + \sqrt{1 - \phi_{\text{Space}}^2} \delta_{a[\mathbf{s}_{c,k}]} \right),$$

where  $a[\mathbf{s}_{c,k}]$  indicates the region that contains the spatial location  $\mathbf{s}_{c,k}$ ,  $\delta_1, \dots, \delta_A \stackrel{\text{iid}}{\sim} \mathcal{N}(0, 1)$ , and  $(v_1, \dots, v_A) \sim \mathcal{N}_A(\mathbf{0}, \mathbf{Q}_{\text{Besag}}^{-1})$ . The combination of these two model components was termed a BYM2 model by Riebler et al. (2016) and has parameters  $\boldsymbol{\theta}_{\text{Space}} = (\sigma_{\text{Space}}^2, \phi_{\text{Space}})$ , but similar choices exist, e.g., in the Leroux model (Leroux et al., 1999). We use a sum-to-zero constraint to avoid confounding with the intercept. In Section 5.1, we also explore using a Matérn Gaussian random field for the main spatial effect – this has been the standard approach so far.

*Spatio-temporal interaction*

Spatial heterogeneity may vary over time, and we include spatio-temporal interaction,

$$\text{Space-Time}(\mathbf{s}_{c,k}, t) = \delta_{a[\mathbf{s}_{c,k}], t}, \quad t = 1, 2, \dots, T,$$

where  $(\delta_{1,1}, \dots, \delta_{A,1}, \delta_{2,1}, \dots, \delta_{A,T}) \sim \mathcal{N}_{AT}(\mathbf{0}, \mathbf{Q}_{\text{intTime}}^{-1} \otimes \mathbf{Q}_{\text{Besag}}^{-1})$  describes a Kronecker combination of a temporal model such as RW1, RW2 or AR(1), and a Besag model in space. The Besag precision matrix is the same as for the main spatial effect, and the model component has parameters  $\theta_{\text{ST}}$  arising from the temporal model in the interaction. To avoid confounding with the main effect in space, we have sum-to-zero constraints  $\sum_{t=1}^T \delta_{a,t} = 0$  for  $a = 1, \dots, A$ . Similarly, to avoid confounding with the main effect in time, we have sum-to-zero constraints  $\sum_{a=1}^A \delta_{a,t} = 0$  for  $t = 1, \dots, T$ . For RW1 and AR(1), a separate area-defined random slope component is needed to capture variation in area-specific linear changes over time; see Section 5.2 for a demonstration.

**4.4. Estimating prevalence across administrative areas**

There is spatial misalignment (Gelfand, 2010) between the desired areal estimates and the point-referenced observations. When the cluster-level model for risk includes spatio-temporal coordinates and covariates, we can only estimate risk at clusters for which this information is known. Furthermore, estimating prevalences at the clusters requires knowledge about the target population sizes at all clusters. We therefore need additional information about the target population to aggregate the clusters and produce areal prevalence estimates. A detailed investigation is ongoing research (Paige et al., 2021).

We demonstrate the issue through a simplified example. Consider the target population in an administrative area indexed by a set of clusters  $c = 1, \dots, M$ , where  $N_c$  and  $Z_c$  denotes the number of individuals and the number of individuals with the outcome of interest, respectively, in cluster  $c$ . Let  $N = N_1 + \dots + N_M$ , then the desired target of inference is the prevalence  $P = \sum_{c=1}^M \frac{N_c}{N} \times \frac{Z_c}{N_c}$ . After a spatial cluster-level model with covariates is estimated based on the survey data, estimating  $P$  would additionally require knowledge about the population sizes, spatial locations, and covariates for every cluster in the administrative area.

Current geostatistical approaches assume that the population in the administrative area is so large that the difference between prevalence and risk is minor. This implies changing the target of inference to  $r = E[P | \{N_c\}_{c=1}^M, \{r_c\}_{c=1}^M] = \sum_{c=1}^M \frac{N_c}{N} \times r_c$ , where  $r_c$  are the cluster-specific risks. However, population sizes are not known, and we are missing the required cluster-specific information to estimate  $r_c$  for unobserved clusters. One solution to overcoming these hurdles has been to replace  $N_c$  by spatially varying population density  $\rho(\cdot)$ , and to replace  $r_c$  by a spatially varying risk  $r_s(\cdot)$ . This gives an approximation of  $r$  by the ratio of two integrals,

$$r_{\text{smooth}} = \frac{\int_{\mathcal{A}} \rho(\mathbf{s}) r_s(\mathbf{s}) d\mathbf{s}}{\int_{\mathcal{A}} \rho(\mathbf{s}) d\mathbf{s}}, \quad (4)$$

where  $\mathcal{A}$  is the geographic area constituting the administrative area. Three key issues need to be investigated: 1) the accuracy of age-specific population surfaces  $\rho(\cdot)$ , 2) the

selection of the *smooth risk surface*  $r_S(\cdot)$ , and 3) under which conditions is  $r_{\text{smooth}} \approx r \approx P$ .

Under the beta-binomial likelihood in Section 4.2, the latent model for risk in Equation (3) can be evaluated at any spatio-temporal location and is the obvious choice for  $r_S(\cdot)$ . However, for the Lono-Binomial likelihood, the choice depends on the interpretation of the cluster-specific random effects. If the cluster-specific effect is measurement error, it should be excluded from  $r_S(\cdot)$ , and if the cluster-specific effect is overdispersion, one should marginalize over it when calculating  $r_S(\cdot)$ . On the other hand, if the cluster-specific effect describes true between-cluster variation, it would be impossible to include it in  $r_S(\cdot)$  unless we knew the exact boundaries of each cluster. The option taken in Paige et al. (2020) is to marginalise the cluster-specific random effect and interpret  $r_S(\cdot)$  as the expected risk under repeated sampling of new clusters at the given location. However, we are also investigating simulation of sampling frames consistent with auxilliary information such as population density and summary information available about the original master sampling frame at coarse scale (Paige et al., 2021).

These issues have received little discussion in the midst of the recent trend of producing fine-scale pixel maps of demographic and health indicators (Giorgi and Diggle, 2017; Burstein et al., 2019). Care should be taken when interpreting the pixel maps and comparing different pixel maps. Dong and Wakefield (2021) provides a more detailed discussion of the different interpretations. In the Lono-Binomial case; some authors have removed the cluster-specific effect in prediction (Wakefield et al., 2019; Diggle and Giorgi, 2019), and others include a new cluster effect in each pixel (Burstein et al., 2019; Utazi et al., 2020). The latter makes the implicit assumption that each pixel constitutes a cluster.

#### 4.5. *Handling urban and rural stratification in prevalence estimation*

Urban/rural rasters that conform with the definition of urban/rural used in different sampling frames do not exist. In this paper, in order to perform aggregation, we propose the following approach to produce pixel-level maps of urban/rural. We assume that we know the correct proportion of urban population over rural population in each admin1 area. When no changes have been made to the sampling frame, these can be found in the survey reports such as for Malawi in Section 5.2, and when the sampling frame has been changed, an updated list must be aquired such as for Nigeria in Section 5.1. We obtained the updated list for NDHS2018 through contact with DHS. The algorithm for producing the urban/rural pixel map is:

1. From WorldPop, download  $100\text{ m} \times 100\text{ m}$  maps of all-age population density for the year matching the list of known urban proportions, and age-specific population density for all years where estimates are desired.
2. For each admin1 area, select a threshold and set pixels with population above the threshold as urban and values below the threshold as rural. The thresholds are selected by using the all-age population density map and matching the urban proportion to the known urban proportion.

3. For each year of interest, combine the urban/rural map with the age-specific population density map for that year in the expression for  $r_{\text{smooth}}$  in Equation (4).

For vaccination coverage, we used the [1, 5) year population, and for NMR, we used the [0, 1) year population. These do not match the desired age-groups exactly, but corresponds to the best granularity available from WorldPop.

#### 4.6. Computation

Inference for complex spatio-temporal Bayesian hierarchical models requires specialized tools. The R package INLA (Lindgren and Rue, 2015; Rue et al., 2017) implements approximate full Bayesian inference using the INLA method (Rue et al., 2009), and the R package TMB (Kristensen et al., 2016) provides empirical Bayesian inference that allows fast inference for spatio-temporal models (Osgood-Zimmerman and Wakefield, 2021). There are also more specific tools such as the R package SUMMER (Li et al., 2021), which extends INLA and produces estimates of prevalence at a specified administrative level, and PrevMap (Giorgi and Diggle, 2017), which produces continuously indexed maps of risk. The power of INLA has been demonstrated in, e.g., Golding et al. (2017); Burstein et al. (2019); Utazi et al. (2020); Bakka et al. (2018), and SUMMER and the Beta-Binomial model was used in Li et al. (2019) and UN IGME (2021). We use INLA in Section 5.1 due to flexibility in exploring new models, and we use SUMMER in Section 5.2 due to the ease of use for prevalence estimation based on household surveys.

### 5. Case studies

#### 5.1. Spatial estimation of vaccination coverage in Nigeria

##### 5.1.1. Modelling at different spatial resolutions

The dataset was described in Section 2.1, and Appendix B provides additional details. There are 1324 clusters that have both GPS coordinates and at least one child in the [12, 24) month age-group. For cluster  $c$  with spatial location  $\mathbf{s}_c$ , we observe  $n_c$  children of which  $y_c$  are vaccinated,  $c = 1, 2, \dots, 1324$ . We use a Lono-Binomial model, where  $Y_c | n_c, R_c \sim \text{Binomial}(n_c, R_c)$  independently for  $c = 1, \dots, 1324$ . The apparent risk  $R_c = \text{expit}(\eta(\mathbf{s}_c) + \epsilon_c)$  consists of a spatial GRF  $\eta(\cdot)$  and random effects  $\epsilon_1, \dots, \epsilon_{1324} | \sigma_C^2 \stackrel{\text{iid}}{\sim} \mathcal{N}(0, \sigma_C^2)$ , where  $\sigma_C^2$  is the cluster variance. The spatial GRF  $\eta(\cdot)$  contains an intercept, a fixed effect for urban versus rural, a spatial effect, and any spatial covariates. We use the symbol  $R_c$  as opposed to  $r_c$  to highlight that  $R_c$  is not necessarily equal to the true risk  $r_c$  of the cluster depending on the interpretation of the cluster effect.

We consider three model-based ways to incorporate spatial variation: a BYM2 model on admin1 areas (Spat-A1), a BYM2 model on admin2 areas (Spat-A2), and a Matérn GRF (Spat-C). The “C” here is to emphasize that this is a continuous spatial model. Additionally, we consider a model with a Matérn GRF and “poverty” (Tatem et al., 2021) and “travel-time to nearest city” (Weiss et al., 2018) as covariates (Spat-Cov). These are spatially varying covariates in the form of high resolution rasters, and are commonly used in risk mapping for LMICs. These covariates resulted in coefficients that were significantly different than zero, and we aim to explore whether they improve areal estimates. More details on the covariates can be found in Section B.2.

In addition to the model-based approaches, we consider direct estimates for the admin1 areas (Dir-A1), and the smoothed direct estimates for the admin1 areas (SDir-A1) as described in Section 3.4. Spat-C, Spat-Cov and Spat-A2 can produce estimates both for admin1 and admin2 areas, while Spat-A1, Dir-A1 and SDir-A1 can only produce estimates for admin1 areas. See Section B.5 for full details on models and priors.

### 5.1.2. Importance of the interpretation of the cluster effect

Let  $M_a$ ,  $a = 1, \dots, A$ , denote the number of EAs in each administrative area. These are on the order of 10000 EAs, and Table B.1 in Appendix B lists them for the 37 admin1 areas in Nigeria. In Section 4.4, we identified three interpretations of the cluster effect in the observation model: measurement error, overdispersion, and true signal. Let  $U_a$  denote the set of EAs in area  $a$  so that  $U = U_1 \cup \dots \cup U_A$  is the set of all EAs. EA  $c' \in U_a$  has spatial location  $\mathbf{s}_{c'}$  and cluster effect  $\epsilon_{c'} | \sigma_C^2 \sim \mathcal{N}(0, \sigma_C^2)$ , and each interpretation of the cluster effect implies a different true risk:

1. **Measurement error:** the true risk is  $r_{c'} = \text{expit}(\eta(\mathbf{s}_{c'}))$ .
2. **True signal:** the true risk is  $r_{c'} = \text{expit}(\eta(\mathbf{s}_{c'}) + \epsilon_{c'})$ .
3. **Overdispersion:** the true risk is  $r_{c'} = \mathbb{E}[\text{expit}(\eta(\mathbf{s}_{c'}) + \epsilon_{c'}) | \eta(\mathbf{s}_{c'})]$ , that is, the marginalized risk with respect to the cluster effect.

Imagine that the observed cluster  $c$  corresponds to EA  $c'$ . Then the apparent risk,  $R_c$ , in the binomial observation model in Section 5.1.1 matches the true risk,  $r_{c'}$ , under the true signal interpretation, but not under the other two interpretations.

Assume that all EAs have the same size and assume that the area  $a$  is so large that the risk matches the prevalence. We approximate the prevalence by  $P_a \approx \sum_{c' \in U_a} r_{c'} / M_a$ . We fit Spat-A1 and use this expression to estimate prevalence under the three interpretations. In Figure 2, the differences between the measurement error and true signal estimates compared to the overdispersion estimates are plotted against the overdispersion estimates and it is clear that there is not much difference between the overdispersion and the true signal interpretations. This is not unexpected since the number of EAs in each area is large, and  $\sum_{c' \in U_a} r_{c'} / M_a$  under the true signal assumption converges to  $\sum_{c' \in U_a} r_{c'} / M_a$  under the overdispersion assumption when  $M_a$  grows to infinity. Therefore, we will use the overdispersion interpretation and not focus on true non-spatial variation between clusters. On the other hand, using the measurement error interpretation gives different results than the two other interpretations, and should only be done when the context justifies this interpretation. The difference between the measurement error interpretation and the overdispersion interpretation is an odd function around  $0.5 = \text{expit}(0)$  because  $\text{expit}(x) - 0.5$  is an odd function around 0.

### 5.1.3. Spatial aggregation

We approximate the risk in area  $a$  using the area  $a$  specific version of (4) with  $\rho(\cdot)$  the population for children aged  $[1, 5)$  years, and  $r_S(\cdot)$  the smooth risk under the overdispersion interpretation. The smooth risk function is described in Section 4.4, and population

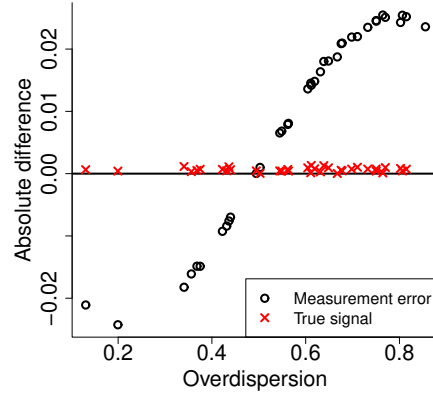


**Figure 2.** For vaccination coverages for the 37 admin1 areas in Nigeria, absolute differences in estimates for different cluster effect interpretations compared to the overdispersion assumption, plotted against estimates under the overdispersion assumption.

density is defined on a  $100\text{ m} \times 100\text{ m}$  with urban/rural assigned according to Section 4.5. Admin1 estimates of prevalence is produced according to the above approach for Spat-A1, Spat-A2, Spat-C, and Spat-Cov, while Dir-A1 and SDir-A1 directly produces estimates of the admin1 prevalences (since they are area-based methods). The point estimates do not vary greatly between the models – the direct estimates are shown in Figure 3 and the estimates from the other models in Figure B.4 in Section B.6. Appendix B also show that the main difference between the admin 1 estimates is that they become smoother as we model at finer spatial scales.

The lengths of the 95% interval estimates for the five models are shown in Figure 4. The direct estimates do not borrow strength across admin1 areas and have the highest uncertainty. Smoothed direct estimates reduces the uncertainty somewhat by post-hoc smoothing of direct estimates across admin1 areas. The biggest reduction in variance happens in areas with high variance, and areas with low variance are not much affected by the post-hoc smoothing. For the four model-based approaches, estimation uncertainty is increasingly reduced as we model at finer and finer spatial scale.

The reduction in variance at finer spatial resolutions warrants further investigation because it may indicate oversmoothing of the sparse data. However, if estimates at finer spatial scales than admin1 areas are desired, Spat-A2, Spat-C and Spat-Cov are the only choice among the six models considered. Figure B.5 gives point and interval estimate widths for admin2 areas for the Spat-A2 and Spat-C models. The estimates and the associated uncertainty for Spat-Cov are qualitatively indistinguishable from Spat-C and are given in Figure B.5 in Appendix B. We see that the point estimates are very similar, while the uncertainty is reduced under the continuous spatial model.

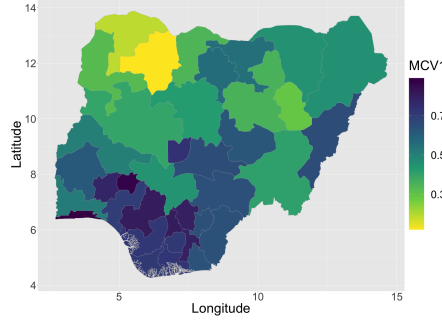


**Figure 3.** Direct estimates of vaccination coverage for the 37 admin1 areas.

#### 5.1.4. Model comparison

The main target of our analysis is prevalences for administrative areas and we aim to assess the models' ability to estimate these. We have sufficient power in the survey to make reliable direct estimates at admin1 areas and propose to view the direct estimates for admin1 areas as observations of the true vaccination coverages in the admin1 areas. From this perspective, the observation model for the logit of the direct estimate in area  $a$ ,  $B_a = \text{logit}(\hat{p}_a)$ , is approximately Gaussian for large sample sizes. The expected value is approximately equal to the true logit of vaccination coverage,  $\text{logit}(p_a)$ , and the estimated variance  $\hat{V}_a$  is computed taking the complex survey design into account.

Each Bayesian model gives rise to a predictive distribution of the true logit vaccination coverage,  $\pi(\text{logit}(p_a)|\text{data})$ . If we hold out clusters in area  $a$  when fitting the model, the direct estimate is independent of the predictive distribution, and we can construct a predictive distribution of the direct estimate,  $\pi(B_a|\text{data from other areas})$ . These can be used in a validation scheme where we compare the 37 hold-out predictive distributions of the direct estimates with the “observed” direct estimates being used to score the predictions. For reference we have included NoSpace, which has a binomial likelihood, and a latent model with separate intercepts for urban and rural, and a cluster effect.

We simplify scoring by assuming that the predictive distributions are Gaussian so that we only need to estimate the posterior mean and posterior standard deviation for each hold-out area. To assess the predictions we use the mean square error (MSE) and the log-score on the logit-scale. Given the normal observation model for the direct estimates, the difference between the MSE and log-score metrics is that the latter scale the sum of squares by the estimated variance of the direct estimates. See Section B.7 for further details. In addition, we compute a coverage for the hold-out areas as the proportion of the 37 direct estimates that are contained in the 95% credible intervals. Table 2 shows that for admin1-level validation, Spat-A2 and Spat-C perform best in terms of MSE, but that they are substantially worse for Log-score. This suggests that while square errors in central predictions are better, the predictive distributions are less compatible with the observed direct estimates. This is supported by the fact that Spat-A2 and Spat-C only have coverages just below 60% compared to SDir-A1 and Spat-A1 that have coverages of 92%. Furthermore, the introduction of covariates in Spat-Cov reduces the coverage to 51%. This suggests that modelling at fine resolution should not be done just because



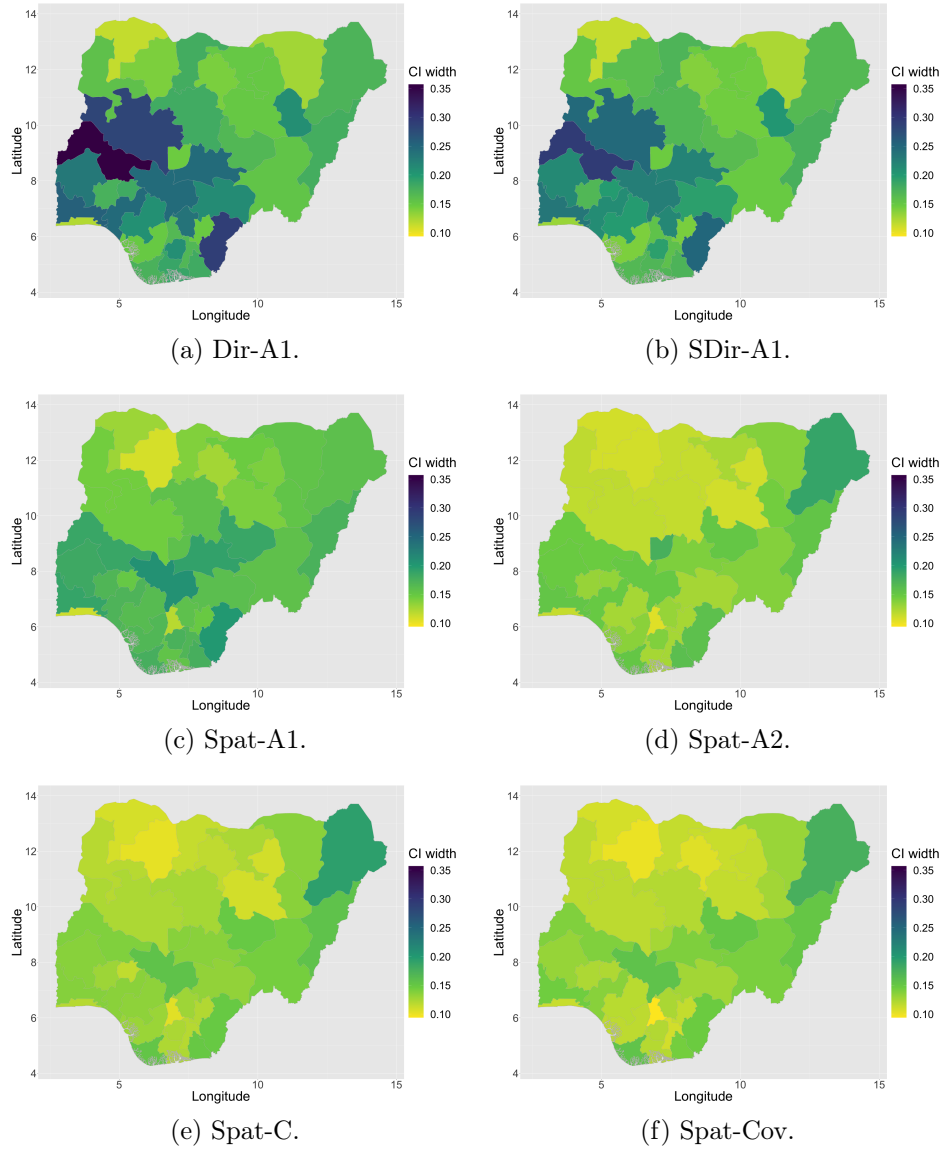


**Figure 4.** The lengths of 95% interval estimates for the six different models, for admin1 areas.

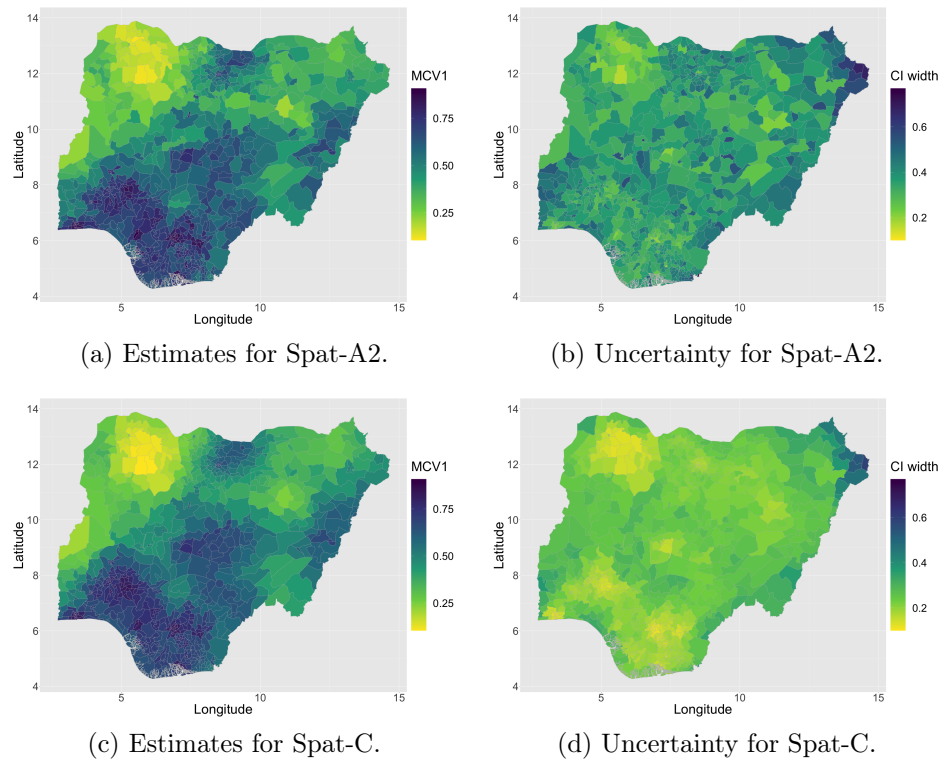


**Figure 5.** Left: Estimated admin2 vaccination coverages under Spat-A2 and Spat-C models. Right: Uncertainty under Spat-A2 and Spat-C models, where uncertainty is quantified by the length of the 95% credible interval.

**Table 2.** Scores for hold-out predictions of direct estimates in the 37 admin1 areas, and 10-fold cross-validation for cluster predictions. Lower scores are better.

	NoSpace	SDir-A1	Spat-A1	Spat-A2	Spat-C	Spat-Cov
<b>Admin1-level</b>						
MSE	0.62	0.44	0.38	0.34	0.36	0.33
Log-score	4.35	0.98	0.92	1.09	1.19	1.11
Coverage (%)	0	92	92	57	59	51
<b>Cluster-level</b>						
MSE	0.109	–	0.089	0.088	0.088	0.087
Log-score	1.52	–	1.40	1.39	1.39	1.39

we have the ability to do so, but that one should keep the target of inference in mind when choosing the model, and that model validation is important. This point of view is supported by Corral et al. (2021) who suggest that random effects should be introduced at the level at which inference is desired.

The added value of admin1-level validation is clear when compared with standard 10-fold cross-validation. Here we randomly divide the 1324 clusters into 10 similarly sized sets, hold-out one set at a time, fit the model to the remaining clusters, and predict the observed vaccination coverage for the hold-out clusters. MSE and log-scores are then computed cluster-wise and averaged across all clusters. Table 2 shows that cluster-level validation can detect that spatial modelling is beneficial, but does not have the power to differentiate between the spatial models due to the low number of trials in each cluster.

## 5.2. Spatio-temporal estimation of NMR in Malawi

### 5.2.1. Choices of temporal smoothing

We now consider the spatio-temporal modeling of yearly NMR in Malawi, from 2000 to 2016, with short term projection to 2019. There are four standard DHS surveys conducted in Malawi during this period. The two early surveys in 2000 and 2004 provide limited information and poses additional challenge of aggregating over two different sets of urban/rural stratification definitions. Thus we focus on the two DHS surveys conducted in 2010 and 2015-2016 described in Section 2.2. Additional details for earlier DHS surveys are included in Appendix C.

The temporal smoothing component in the model plays a central role in short-term projection. We first consider a national model to gauge the overall temporal trend of NMR in Malawi. For cluster  $c$  in survey  $k$ , we observe  $Y_{c,t,k}$  neonatal deaths and  $n_{c,t,k}$  births in year  $t$ . We use a Beta-Binomial model with  $Y_{c,t,k}|r_{c,t,k}, n_{c,t,k}, d \sim \text{Beta-Binomial}(n_{c,t,k}, r_{c,t,k}, d)$  and risk  $r_{c,t,k} = \eta(\mathbf{s}_{c,k}, t) + \alpha_k = \mu_{\text{Urb}[c,k]} + \gamma_{\text{Urb}[c,k],t} + \nu_t + \alpha_k$  for  $t = 1, \dots, T$  and  $k = 1, 2$ , where  $\nu_t|\sigma_\nu^2 \stackrel{\text{iid}}{\sim} \mathcal{N}(0, \sigma_\nu^2)$  is an unstructured random effect for temporal shocks. The survey and temporal main effects are parameterized as described in Section 4.3. Figure 6 shows the comparison of posterior median and 95% credible intervals of the stratum-specific NMR at the national level following the three parameterizations discussed in Section 4.3: a RW2 model, a RW1 model with shared linear trend, and an AR(1) model with shared linear trend. The different choices of the temporal component lead to different projections and uncertainties after 2015. The

RW2 projections quickly become very wide, and do not seem useful or realistic. The RW1 model simply keeps the estimated urban and rural deviations from the main trend in the last time period constant in the projection with increasing uncertainties. In the context of modeling NMR in Malawi, treating the urban and rural trends as independent random walks may not be ideal as the fraction of the population that is urban is small and neonatal deaths are relatively rare. Thus the temporal trends are more likely to be influenced by the sparse data in the last few years. Therefore, we prefer the AR(1) model with shared linear trends across the two strata. Under this model, the projections for both urban and rural NMR will converge to the shared linear trend. This is a reasonable assumption given the limited data.

We also combine the stratum-specific estimates using national urban/rural fractions calculated using the procedure described in Section 4.5. Detailed steps are presented in the Appendix C. Figure 6 also shows the comparison between the three projections of national NMR with the UN-IGME estimates (and also the observed data, in the form of national weighted estimates). The UN-IGME estimates are produced by the B3 model developed in Alkema and New (2014) and use data sources going back to 1970. The stronger trend of decline in the UN-IGME projections is driven mostly by observations before 2000. Our analysis of the latest two surveys, however, seem to suggest a more stagnant trend of NMR in the last 20 years, which is consistent with the Malawi DHS report and other literature (e.g., Lungu et al., 2019). In general, forming projections with limited data is a difficult task and depends on the analysis context. Scenario-based analyses with various forecasting models that encode different assumptions for the future may be a useful tool for policymakers. For example, we could fix the slope of the linear trends after 2015 to different levels, leading to projections with less uncertainty but under different scenarios. We would not average over the different scenarios, however, since this offers the mirage of “averaging over scenario uncertainty”, which is dangerous since there are many different scenarios that could be considered and only a limited number will ever be presented/considered.

### 5.2.2. *Estimates of subnational NMR*

We fit the subnational Beta-Binomial model described in Section 4.2 with  $\gamma_{\text{Urb}[c,k],t}$  modeled as two separate AR(1) process with shared linear trends in time. For the prior on the space-time interaction term, we adopt the Gaussian prior with a precision matrix using the Kronecker combination of precision matrices from an AR(1) model in time and a Besag model in space. We also include a random slope in time for each area. Detailed model specification is provided in the Appendix C. The time-varying odds ratios associated with clusters in the urban partition are represented by  $\exp(\mu_1 + \gamma_{1,t}) / \exp(\mu_0 + \gamma_{0,t})$  and visualizations of the odds ratio is included in Appendix C. The posterior median and the 95% credible intervals of NMR over time are shown in Figure 7. To compare with the design-based estimates, we compute direct estimates of NMR at 4-year intervals from 2000–2003 to 2012–2005 using both DHS surveys. There is strong smoothing from the Beta-Binomial models, which is expected from the very sparse data. The estimates from the smoothed direct model is very similar and is included in Appendix C. Figure 8 shows the posterior median of NMR on the Malawi map for a subset of the years in

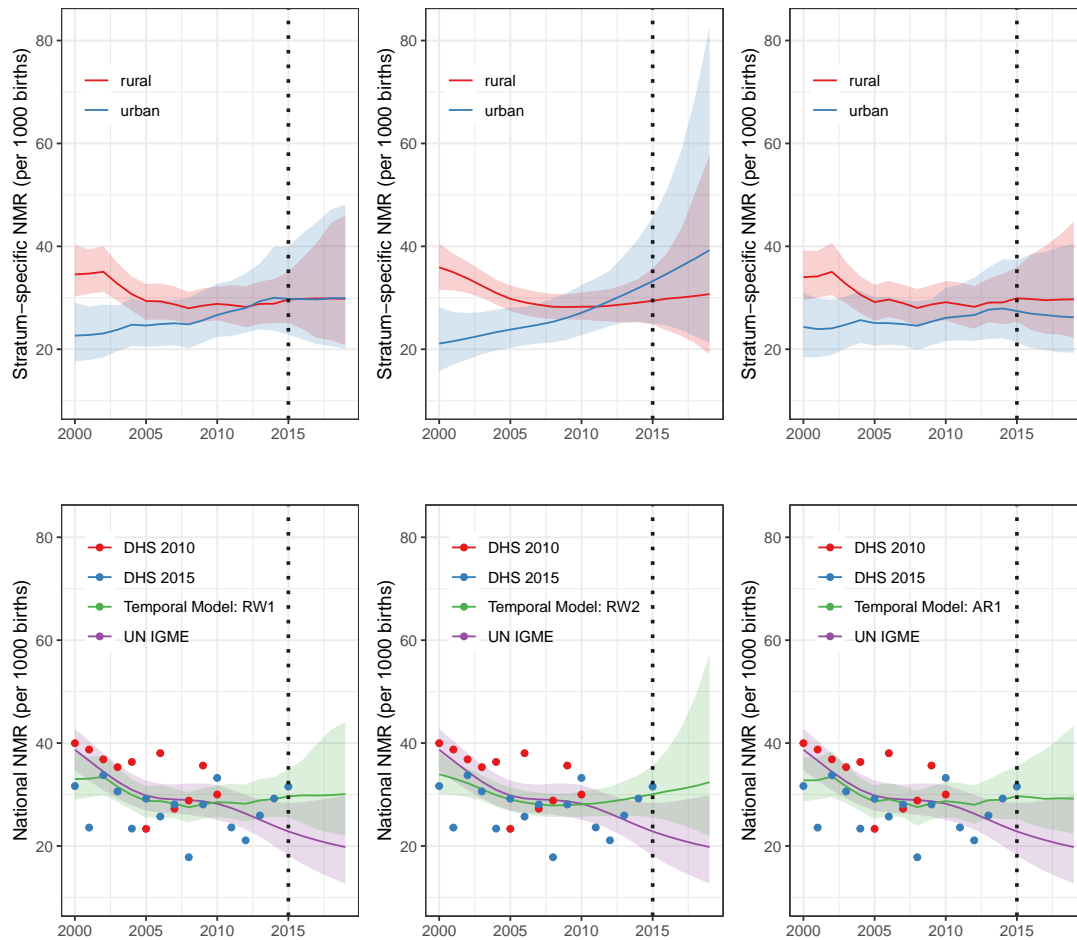


**Figure 6.** Estimates of national NMR in Malawi using different temporal smoothing models. Color ribbons correspond to 95% credible intervals. Top row: national NMR by urban/rural strata. Bottom row: aggregated national NMR, comparing to the direct estimates from the two surveys and the UN IGME estimates. Three temporal models are used. Left: RW1 with shared linear trend. Middle: RW2. Right: AR(1) with shared linear trend. Vertical dots are at the last data collection time.



**Figure 7.** The posterior median and 95% credible interval of NMR in the 28 districts of Malawi with comparison to direct estimates at 4-year intervals from the two DHS surveys.

the analysis. The spatial distribution of NMR does not change dramatically over time. Appendix C contains distributions on the rankings of the 28 districts.

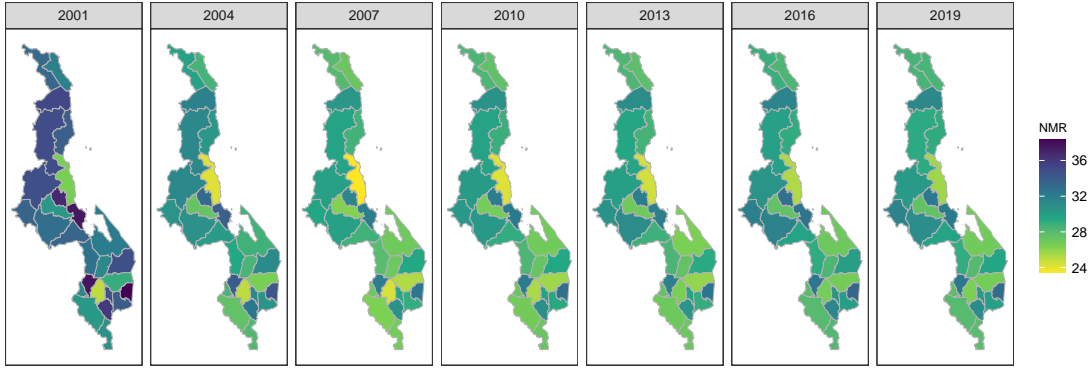


**Figure 8.** The posterior median of NMR in the 28 districts of Malawi in selected years.

## 6. Discussion

Subnational prevalence mapping entails the estimation of empirical proportions in administrative areas. Traditional SAE approaches directly target such proportions and estimation is intimately connected to the survey design under which the data was collected. However, successful application of these approaches hinges on sufficient power for direct estimation or sufficient power for indirect estimation through reliable auxiliary population information at the target resolution. This means that unit-level models cannot include spatial effects at finer resolutions than one has population sizes. For example, a cluster-level spatial effect requires knowledge about the locations and the population sizes of all EAs in order to predict the outcomes of the unobserved individuals in a consistent way. Thus, the SAE literature does not typically go beyond simple unstructured random effects or area-level random effects when modeling between-area variation.

Traditional geostatistical approaches take a different perspective. Models are expressed in terms of risk with the aim being to describe the outcome at any spatial location. Since the data source is point-referenced, this motivates the use of spatial models in continuous space. Such models have the potential to provide detailed maps of the spatial variation in risk, but areal estimates cannot be produced without detailed auxiliary population information and one has to consider the sampling design.

There is a strong and growing desire to produce official subnational estimates of demographic and health indicators. When producing official statistics using SAE, Tzavidis et al. (2018) suggest that one consider progressively finer geographies while at each level assessing the feasibility of producing SAE estimates for the current level. In our experience, for estimation when the data are rich, for example when constructing national estimates using DHS or MICS surveys, direct (weighted) estimation is a reliable approach. This offers asymptotic (design) consistency and the inclusion probabilities encompass all the necessary information to estimate a national prevalence. The weighted estimates implicitly encode the relevant population information (the weights were con-

structed from the sampling frame), and target empirical proportions. In the context of LMICs, reliable covariate information is limited, and at admin1 one should first consider areal Fay-Herriot SAE models such as Mercer et al. (2015), and if the survey does not provide reliable admin1 estimates using SAE, one should apply spatial smoothing. For finer levels such as admin2 or pixel maps, one should generally use spatial statistical methods, but ensure that the model contains terms to acknowledge the complex design. The key point here is that the goal of the analysis should determine the approach, and different goals may call for different approaches.

Complex survey designs lead to spatially varying sampling efforts. This resembles geostatistical preferential sampling (Diggle et al., 2010), but in survey sampling, the inclusion probabilities are not directly linked to the level of risk in the clusters. The inclusion probabilities are instead determined by a survey design that aims to reach the desired statistical power for areas of interest in a cost efficient way. This does not mean that the survey design should be haphazardly ignored, however. Most household surveys are stratified on the basis of urban/rural, and it is commonplace for the outcome to be associated with this classification. We have chosen to acknowledge the stratification in spatial models using covariates and area effects.

Aggregation is a major challenge even without the presence of a complex survey design. For example, if one disaggregates areas into rural and urban, it is necessary to come up with reliable aggregation weights for combining the rural and urban estimates in each area. Estimating an urban/rural association is relatively uncomplicated, but producing reliable fine-scale maps of urban/rural, which are needed for spatial aggregation, is an ongoing research problem. Treating space as continuous, increases the challenge as one needs to rely on fine-scale population density rasters to perform aggregation to the areal level. Both population and covariate rasters are estimated based on other data sources, and there is need for further investigation to understand the consequences of not acknowledging the inherent uncertainty when using them in an aggregation scheme. The result of aggregation is typically an areal risk and an examination of the importance of distinguishing between risk and prevalence at different spatial scales would be worthwhile. These open issues motivate our suggestion for spatial modelling at the target administrative level unless the stratification necessitates modelling at finer scales. Corral et al. (2021) reached a similar conclusion.

Section 5.2 demonstrates the clear importance of model choices both in terms of central predictions and uncertainty. Since it will always be possible to argue for many reasonable models, we need formal validation techniques to compare different models in terms of their ability to estimate areal prevalences. However, the spatial misalignment between the point-referenced observations and the desired areal quantities makes validation a challenging task. We propose a model validation approach that frames direct estimates as observations and scores different models based on their ability to predict direct estimates. One should be wary of using more complex models unless one can show they are better than simpler models through validation. In the case study, we observe that modelling at finer spatial scales than the target administrative level, gave rise to poorer prediction scores. In particular, a continuously-indexed risk surface performed more poorly than a model with constant risk in each administrative area. As an extreme example, if we wanted a national estimate, we would not use spatial mod-



els and aggregate, but simply calculate a weighted estimate. There are cases in which a continuously-indexed model is necessary for a principled way to handle data that is available with limited geographical information (e.g., area only information and not points) or under different geographical partitions (Marquez and Wakefield, 2021; Wilson and Wakefield, 2020).

There are several other important aspects that have not been addressed in this paper, and require further research. In particular, spatio-temporal analysis may require the combination of surveys from different sampling frames. This further complicates the issue of urban/rural stratification because the definitions of urban/rural in the sampling frames will most likely give rise to different geographic stratifications. One may then stratify the model by urban/rural crossed by sampling frame, but the question is how to combine estimates for different sampling frames into a single estimate? Additionally, a common technique in survey statistics is poststratification whereby inclusion probabilities are adjusted to account for known structures in the population such as the proportion of males to females. It is not obvious how to adjust the aggregation schemes in a similar way for geostatistical models, but poststratification is less common in LMICs since such information is typically lacking. The fact that the GPS coordinates provided to the public have been jittered is another source for concern, but the amount is always small compared to the size of a country. Finally, benchmarking the subnational estimates to officially accepted national levels may be necessary (Särndal, 2007; Zhang and Bryant, 2020), and non-sampling errors such as recollection bias and migration of interview subjects may bias estimates.

A more complex, but unstratified, version of the model described in Section 4.2 and applied in Section 5.2 has been used to produce spatio-temporal estimates of U5MR for 22 LMICs (UN IGME, 2021). A key focus for these estimates was to consider each country separately, rather than a joint model for multiple countries (as practiced by IHME, see for example, Burstein et al. (2018)). This is important as some countries require specific considerations such as adjustments due to natural disasters or conflicts. There is still work to be done in making such estimates a tool that routinely guides policy decisions. We believe a key focus should be on transparent methods and software such as **SUMMER** (Li et al., 2021) that can be reproducibly run by national statistics' offices. Software should be accompanied with development of detailed vignettes. This is consistent with the GATHER statement (Stevens et al., 2016). We have recently partnered with researchers at DHS to produce guidelines and code scripts to routinely produce subnational child mortality estimates (Wu et al., 2021).

We believe that the way forward for prevalence mapping is to bridge the rich literatures of SAE and spatial statistics. The aim should be a synthesis which exploits the broad range of techniques from spatial statistics to overcome data sparsity, but at the same time acknowledges the design and the subnational areal targets of inference, which are often empirical averages. As a step in this direction, we have presented an approach that is framed from a spatial statistics perspective, but includes cluster effects to acknowledge clustering, and urban/rural fixed effects and a piece-wise constant risk surface to acknowledge stratification. The latter is similar to the inclusion of fixed effects to acknowledge stratification, but induces spatial smoothing. The approach is not fully design-consistent, and does not capture all aspects of the inclusion probabilities or make

non-response adjustments. However, we believe it is an important step towards spatial modelling with a clear understanding of the importance of the survey design, which has too often been downplayed.

## Acknowledgments

We are grateful to the Space Time Analysis Bayes (STAB) working group for discussion and feedback on the paper. We also acknowledge the DHS for access and use of the data, and for permission to make available the cluster aggregates and their displaced locations.

## References

- Alexander, M. and Alkema, L. (2018). Global estimation of neonatal mortality using a Bayesian hierarchical splines regression model. *Demographic Research*, 38:335–372.
- Alkema, L. and New, J. (2014). Global estimation of child mortality using a Bayesian B-spline bias-reduction model. *The Annals of Applied Statistics*, 8:2122–2149.
- Bakka, H., Rue, H., Fuglstad, G.-A., Riebler, A., Bolin, D., Illian, J., Krainski, E., Simpson, D., and Lindgren, F. (2018). Spatial modeling with r-inla: A review. *WIREs Computational Statistics*, 10:e1443.
- Battese, G. E., Harter, R. M., and Fuller, W. A. (1988). An error-components model for prediction of county crop areas using survey and satellite data. *Journal of the American Statistical Association*, 83:28–36.
- Besag, J., York, J., and Mollié, A. (1991). Bayesian image restoration with two applications in spatial statistics. *Annals of the Institute of Statistics and Mathematics*, 43:1–59.
- Breidt, J. and Opsomer, J. (2017). Model-assisted survey estimation with modern prediction techniques. *Statistical Science*.
- Burstein, R., Henry, N. J., Collison, M. L., Marczak, L. B., Sligar, A., Watson, S., Marquez, N., Abbasalizad-Farhangi, M., Abbasi, M., Abd-Allah, F., et al. (2019). Mapping 123 million neonatal, infant and child deaths between 2000 and 2017. *Nature*, 574:353–358.
- Burstein, R., Wang, H., Reiner Jr, R. C., and Hay, S. I. (2018). Development and validation of a new method for indirect estimation of neonatal, infant, and child mortality trends using summary birth histories. *PLoS Medicine*, 15:e1002687.
- Corral, P., Himelein, K., McGee, K., and Molina, I. (2021). A map of the poor or a poor map? Policy Research Working Paper;No. 9620, World Bank, Washington, DC.
- Cressie, N. and Wikle, C. (2011). *Statistics for Spatio-Temporal Data*. John Wiley and Sons.
- Datta, G. S., Kubokawa, T., Molina, I., and Rao, J. (2011). Estimation of mean squared error of model-based small area estimators. *Test*, 20:367–388.

- Diggle, P. and Giorgi, E. (2016). Model-based geostatistics for prevalence mapping in low-resource settings. *Journal of the American Statistical Association*, 111:1096–1120.
- Diggle, P. J. and Giorgi, E. (2019). *Model-based Geostatistics for Global Public Health: Methods and Applications*. Chapman and Hall/CRC, Boca-Raton.
- Diggle, P. J., Menezes, R., and Su, T.-L. (2010). Geostatistical inference under preferential sampling. *Journal of the Royal Statistical Society: Series C*, 59:191–232.
- Dong, T. and Wakefield, J. (2021). Modeling and presentation of health and demographic indicators in a low- and middle-income countries context. *Vaccine*, 39:2584–2594.
- Fay, R. and Herriot, R. (1979). Estimates of income for small places: an application of James–Stein procedure to census data. *Journal of the American Statistical Association*, 74:269–277.
- Fuglstad, G.-A., Simpson, D., Lindgren, F., and Rue, H. (2019). Constructing priors that penalize the complexity of Gaussian random fields. *Journal of the American Statistical Association*, 114:445–452.
- Gelfand, A. (2010). Misaligned spatial data. In Gelfand, A., Diggle, P., Fuentes, M., and Guttorp, P., editors, *Handbook of Spatial Statistics*, pages 517–539. CRC Press.
- Gelman, A. and Hill, J. (2006). *Data Analysis using Regression and Multilevel/Hierarchical Models*. Cambridge University Press.
- General Assembly of the United Nations (2015). Resolution adopted by the General Assembly on 25 September 2015. A/RES/70/1.
- Giorgi, E. and Diggle, P. J. (2017). Prevmap: An r package for prevalence mapping. *Journal of Statistical Software, Articles*, 78:1–29.
- Golding, N., Burstein, R., Longbottom, J., Browne, A., Fullman, N., Osgood-Zimmerman, A., Earl, L., Bhatt, S., Cameron, E., Casey, D., Dwyer-Lindgren, L., Farag, T., Flaxman, A., Fraser, M., Gething, P., Gibson, H., Graetz, N., Krause, L., Kulikoff, X., Lim, S., Mappin, B., Morozoff, C., Reiner, R., Sligar, A., Smith, D., Wang, H., Weiss, D., Murray, C., Moyes, C., and Hay, S. (2017). Mapping under-5 and neonatal mortality in Africa, 2000–15: a baseline analysis for the Sustainable Development Goals. *The Lancet*, 390:2171–2182.
- Hájek, J. (1971). Discussion of, “An essay on the logical foundations of survey sampling, part I”, by D. Basu. In Godambe, V. and Sprott, D., editors, *Foundations of Statistical Inference*. Holt, Rinehart and Winston, Toronto.
- Horvitz, D. and Thompson, D. (1952). A generalization of sampling without replacement from a finite universe. *Journal of the American Statistical Association*, 47:663–685.
- Hosseinpour, A. R., Bergen, N., Barros, A. J., Wong, K. L., Boerma, T., and Victora, C. G. (2016). Monitoring subnational regional inequalities in health: measurement approaches and challenges. *International Journal for Equity in Health*, 15:1–13.

- ICF International (2012). *Demographic and Health Survey Sampling and Household Listing Manual*. MEASURE DHS, MD: Claverton.
- Knorr-Held, L. (2000). Bayesian modelling of inseparable space-time variation in disease risk. *Statistics in Medicine*, 19:2555–2567.
- Kristensen, K., Nielsen, A., Berg, C. W., Skaug, H., and Bell, B. M. (2016). TMB: Automatic differentiation and laplace approximation. *Journal of Statistical Software, Articles*, 70:1–21.
- Lehtonen, R. and Veijanen, A. (2009). Design-based methods of estimation for domains and small areas. In *Handbook of statistics*, volume 29, pages 219–249. Elsevier.
- Leroux, B., Lei, X., and Breslow, N. (1999). Estimation of disease rates in small areas: A new mixed model for spatial dependence. In Halloran, M. and Berry, D., editors, *Statistical Models in Epidemiology, the Environment and Clinical Trials*, pages 179–192. Springer, New York.
- Li, Z., Hsiao, Y., Godwin, J., Martin, B. D., Wakefield, J., Clark, S. J., with support from the United Nations Inter-agency Group for Child Mortality Estimation, and its technical advisory group (2019). Changes in the spatial distribution of the under-five mortality rate: Small-area analysis of 122 DHS surveys in 262 subregions of 35 countries in Africa. *PloS one*, 14:e0210645.
- Li, Z. R., Martin, B. D., Dong, T. Q., Fuglstad, G.-A., Paige, J., Riebler, A., Clark, S., and Wakefield, J. (2020). Space-time smoothing of demographic and health indicators using the R package SUMMER. *arXiv preprint arXiv:2007.05117*.
- Li, Z. R., Martin, B. D., Hsiao, Y., Godwin, J., Paige, J., Wakefield, J., Clark, S. J., Fuglstad, G.-A., and Riebler, A. (2021). *SUMMER: SAE Unit/area Models and Methods for Estimation in R*. R package version 1.2.0.
- Lindgren, F. and Rue, H. (2015). Bayesian spatial modelling with R-INLA. *Journal of Statistical Software*, 63:1–25.
- Lindgren, F., Rue, H., and Lindström, J. (2011). An explicit link between Gaussian fields and Gaussian Markov random fields: the stochastic differential equation approach (with discussion). *Journal of the Royal Statistical Society, Series B*, 73:423–498.
- Little, R. J. (2003). The Bayesian approach to sample survey inference. In *Analysis of survey data*, pages 49–57. Wiley Online Library.
- Local Burden of Disease Vaccine Coverage Collaborators and others (2021). Mapping routine measles vaccination in low-and middle-income countries. *Nature*, 589:415.
- Lohr, S. (2009). *Sampling: Design and Analysis*. Cengage Learning.
- Lumley, T. (2004). Analysis of complex survey samples. *Journal of Statistical Software*, 9:1–19.
- Lumley, T. (2018). *survey: analysis of complex survey samples*. R package version 3.35.

- Lungu, E. A., Biesma, R., Chirwa, M., and Darker, C. (2019). Is the urban child health advantage declining in malawi?: evidence from demographic and health surveys and multiple indicator cluster surveys. *Journal of Urban Health*, 96:131–143.
- Malawi National Statistical Office (2008). Population and housing census results. [http://www.nsomalawi.mw/index.php?option=com\\_content&view=article&id=107%3A2008-population-and-housing-census-results&catid=8&Itemid=6](http://www.nsomalawi.mw/index.php?option=com_content&view=article&id=107%3A2008-population-and-housing-census-results&catid=8&Itemid=6).
- Marhuenda, Y., Molina, I., and Morales, D. (2013). Small area estimation with spatio-temporal Fay–Herriot models. *Computational Statistics and Data Analysis*, 58:308–325.
- Marquez, N. and Wakefield, J. (2021). Harmonizing child mortality data at disparate geographic levels. *Statistical Methods in Medical Research*, 30:1187–1210.
- Mercer, L., Wakefield, J., Pantazis, A., Lutambi, A., Mosanja, H., and Clark, S. (2015). Small area estimation of childhood mortality in the absence of vital registration. *Annals of Applied Statistics*, 9:1889–1905.
- Mosser, J. F., Gagne-Maynard, W., Rao, P. C., Osgood-Zimmerman, A., Fullman, N., Graetz, N., Burstein, R., Updike, R. L., Liu, P. Y., Ray, S. E., et al. (2019). Mapping diphtheria-pertussis-tetanus vaccine coverage in africa, 2000–2016: a spatial and temporal modelling study. *The Lancet*, 393:1843–1855.
- National Population Commission - NPC and ICF (2019). Nigeria demographic and health survey 2018 - final report. <http://dhsprogram.com/pubs/pdf/FR359/FR359.pdf>.
- National Statistical Office - NSO/Malawi and ICF Macro (2011). Malawi demographic and health survey 2010. <http://dhsprogram.com/pubs/pdf/FR247/FR247.pdf>.
- National Statistical Office/Malawi and ICF (2017). Malawi demographic and health survey 2016-16. <http://dhsprogram.com/pubs/pdf/FR319/FR319.pdf>.
- Osgood-Zimmerman, A. and Wakefield, J. (2021). A statistical introduction to template model builder: A flexible tool for spatial modeling. *arXiv preprint arXiv:2103.09929*.
- Paige, J., Fuglstad, G.-A., Riebler, A., and Wakefield, J. (2020). Design- and model-based approaches to small-area estimation in a low and middle income country context: Comparisons and recommendations. *Journal of Survey Statistics and Methodology*. In press.
- Paige, J., Fuglstad, G.-A., Riebler, A., and Wakefield, J. (2021). Spatial aggregation with respect to a population distribution. In preparation.
- Pfeffermann, D. (1993). The role of sampling weights when modeling survey data. *International Statistical Review / Revue Internationale de Statistique*, 61:317–337.
- Rao, J. and Molina, I. (2015). *Small Area Estimation, Second Edition*. John Wiley, New York.

- Riebler, A., Sørbye, S., Simpson, D., and Rue, H. (2016). An intuitive Bayesian spatial model for disease mapping that accounts for scaling. *Statistical Methods in Medical Research*, 25:1145–1165.
- Rue, H., Martino, S., and Chopin, N. (2009). Approximate Bayesian inference for latent Gaussian models using integrated nested Laplace approximations (with discussion). *Journal of the Royal Statistical Society, Series B*, 71:319–392.
- Rue, H., Riebler, A., Sørbye, S. H., Illian, J. B., Simpson, D. P., and Lindgren, F. K. (2017). Bayesian computing with inla: A review. *Annual Review of Statistics and Its Application*, 4:395–421.
- Särndal, C.-E. (2007). The calibration approach in survey theory and practice. *Survey Methodology*, 33:99–119.
- Scott, A. and Smith, T. (1969). Estimation in multi-stage surveys. *Journal of the American Statistical Association*, 64:830–840.
- Simpson, D., Rue, H., Riebler, A., Martins, T., and Sørbye, S. (2017). Penalising model component complexity: A principled, practical approach to constructing priors (with discussion). *Statistical Science*, 32:1–28.
- Sørbye, S. and Rue, H. (2014). Scaling intrinsic Gaussian Markov random field priors in spatial modelling. *Spatial Statistics*, 8:39–51.
- Stevens, G. A., Alkema, L., Black, R. E., Boerma, J. T., Collins, G. S., Ezzati, M., Grove, J. T., Hogan, D. R., Hogan, M. C., Horton, R., et al. (2016). Guidelines for accurate and transparent health estimates reporting: the GATHER statement. *PLoS medicine*, 13:e1002056.
- Sugden, R. A. and Smith, T. M. F. (1984). Ignorable and informative designs in survey sampling inference. *Biometrika*, 71:495–506.
- Sørbye, S. H. and Rue, H. (2017). Penalised complexity priors for stationary autoregressive processes. *Journal of Time Series Analysis*, 38:923–935.
- Takahashi, S., Metcalf, C. J. E., Ferrari, M. J., Tatem, A. J., and Lessler, J. (2017). The geography of measles vaccination in the african great lakes region. *Nature communications*, 8:15585.
- Tatem, A., Gething, P., Bhatt, S., Weiss, D., and Pezzulo, C. (2021). Nigeria 1km Poverty. <https://www.worldpop.org/geodata/summary?id=1267>. Accessed: 2021-10-18.
- Tzavidis, N., Zhang, L.-C., Luna, A., Schmid, T., and Rojas-Perilla, N. (2018). From start to finish: a framework for the production of small area official statistics. *Journal of the Royal Statistical Society, Series A*, 181:927–979.
- UN IGME (2021). *Subnational Under-five Mortality Estimates, 1990–2019: Estimates developed by the United Nations Inter-agency Group for Child Mortality Estimation*. United Nations Children’s Fund, NY:New York.

- UN System Chief Executives Board for Coordination (2017). Equality and non-discrimination at the heart of sustainable development: A shared united nations framework for action.
- Utazi, C. E., Nilsen, K., Pannell, O., Dotse-Gborgbortsi, W., and Tatem, A. J. (2021). District-level estimation of vaccination coverage: Discrete vs continuous spatial models. *Statistics in Medicine*, 40:2197–2211.
- Utazi, C. E., Thorley, J., Alegana, V. A., Ferrari, M. J., Nilsen, K., Takahashi, S., Metcalf, C. J. E., Lessler, J., and Tatem, A. J. (2018a). A spatial regression model for the disaggregation of areal unit based data to high resolution grids with application to vaccination coverage mapping. *Statistical Methods in Medical Research*, 28:1–16.
- Utazi, C. E., Thorley, J., Alegana, V. A., Ferrari, M. J., Takahashi, S., Metcalf, C. J. E., Lessler, J., Cutts, F. T., and Tatem, A. J. (2019). Mapping vaccination coverage to explore the effects of delivery mechanisms and inform vaccination strategies. *Nature communications*, 10:1–10.
- Utazi, C. E., Thorley, J., Alegana, V. A., Ferrari, M. J., Takahashi, S., Metcalf, C. J. E., Lessler, J., and Tatem, A. J. (2018b). High resolution age-structured mapping of childhood vaccination coverage in low and middle income countries. *Vaccine*, 36:1583–1591.
- Utazi, C. E., Wagai, J., Pannell, O., Cutts, F. T., Rhoda, D. A., Ferrari, M. J., Dieng, B., Oteri, J., Danovaro-Holliday, M. C., Adeniran, A., et al. (2020). Geospatial variation in measles vaccine coverage through routine and campaign strategies in Nigeria: Analysis of recent household surveys. *Vaccine*, 38:3062–3071.
- Wakefield, J., Fuglstad, G.-A., Riebler, A., Godwin, J., Wilson, K., and Clark, S. (2019). Estimating under five mortality in space and time in a developing world context. *Statistical Methods in Medical Research*, 28:2614–2634.
- Watjou, K., Faes, C., Lawson, A., Kirby, R., Aregay, M., Carroll, R., and Vandendijck, Y. (2017). Spatial small area smoothing models for handling survey data with nonresponse. *Statistics in Medicine*, 36:3708–3745.
- Weiss, D. J., Nelson, A., Gibson, H., Temperley, W., Peedell, S., Lieber, A., Hancher, M., Poyart, E., Belchior, S., Fullman, N., et al. (2018). A global map of travel time to cities to assess inequalities in accessibility in 2015. *Nature*, 553:333–336.
- Wilson, K. and Wakefield, J. (2020). Pointless spatial modeling. *Biostatistics*, 21:e17–e32.
- Wu, Y., Li, Z. R., Mayala, B., Wang, H., Gao, P., Paige, J., Fuglstad, G.-A., Moe, C., Godwin, J., Donohue, R., Janocha, B., Croft, T., and Wakefield, J. (2021). Spatial modeling for subnational administrative level 2 small-area estimation. Technical report, ICF International. DHS Spatial Analysis Reports No. 21.
- You, Y. and Zhou, Q. M. (2011). Hierarchical Bayes small area estimation under a spatial model with application to health survey data. *Survey Methodology*, 37:25–37.
- Zhang, J. L. and Bryant, J. (2020). Fully Bayesian benchmarking of small area estimation models. *Journal of Official Statistics*, 36:197–223.

## A. Spatio-temporal cluster-level models

This section provides supplementary details for the latent model described in Equation (3) in Section 4.2.2. Throughout, we let  $c = 1, \dots, M_k$  denotes clusters in survey  $k = 1, \dots, K$ , and we let  $t = 1, \dots, T$  denote time. Furthermore,  $\mathbf{s}_{c,k}$  will be the location of cluster  $c$  in survey  $k$ . The latent risk  $\eta_{c,t,k}$  is modelled by

$$\eta_{c,t,k} = \mu + \text{Covariates}(c, t, k) + \text{Survey}(k) \\ + \text{Time}(t) + \text{Space}(\mathbf{s}_{c,k}) + \text{Space-Time}(\mathbf{s}_{c,k}, t).$$

### A.1. The intercept and covariates

The covariate part of the latent model is given by

$$\eta_{c,t,k} = \mu + \text{Covariates}(c, t, k),$$

and combines a joint intercept  $\mu$  and cluster-specific covariates. The intercept commonly has a vague prior such as  $\mu \sim \mathcal{N}(0, 1000)$ . We consider modelling with the purpose of producing areal estimates or point predictions, and assume that the covariates will be available as spatial rasters. We can then write the contribution of the covariates as

$$\text{Covariates}(c, t, k) = \mathbf{z}(\mathbf{s}_{c,k}, t)^T \boldsymbol{\beta},$$

where  $\mathbf{z}(\cdot, \cdot)$  is  $k$ -dimensional vector of covariates that vary across space and time, and  $\boldsymbol{\beta}$  is a  $k$ -dimensional vector of coefficients. Under the assumption that the covariates are scaled to be around 1, the standard approach is a vague prior  $\boldsymbol{\beta} \sim \mathcal{N}_k(\mathbf{0}, 1000\mathbf{I}_k)$ .

### A.2. The survey effect

The purpose of a survey effect is to account for survey-specific conditions that result in bias relative to the true risk. Under the assumption that these biases are random, a simple model is separate effects for each survey

$$\text{Survey}(k) = \alpha_k,$$

where  $\alpha_k$  is the survey-specific adjustment. There are typically few surveys so that there is little information to learn about the variance of the survey effects. A pragmatic approach is to fix a  $V > 0$  and use the prior  $\alpha_1, \dots, \alpha_K \stackrel{\text{iid}}{\sim} \mathcal{N}(0, V)$ . We enforce the constraint  $\alpha_1 + \dots + \alpha_K = 0$  to make it identifiable together with the joint intercept.

### A.3. The main temporal effect

The main temporal effect aims to capture overall changes in risk at the national level. We write

$$\text{Time}(t) = \gamma_t,$$

where  $\boldsymbol{\gamma} = (\gamma_1, \dots, \gamma_T) | \boldsymbol{\theta}_{\text{time}} \sim \mathcal{N}(\mathbf{0}, \mathbf{Q}_{\text{time}}(\boldsymbol{\theta}_{\text{time}})^{-1})$ . If  $\mathbf{Q}_{\text{time}}(\boldsymbol{\theta}_{\text{time}})$  is singular, this must be understood as an intrinsic distribution. There are several options for the main



temporal effect, but three common choices are an autoregressive process, a first-order random walk and a second-order random walk.

An autoregressive process of order 1 requires a variance parameter,  $\sigma_{\text{time}}^2$ , and an autocorrelation parameter,  $\rho_{\text{time}}$ . We let  $\boldsymbol{\theta}_{\text{time}} = (\sigma_{\text{time}}^2, \rho_{\text{time}})$ . The temporal evolution can be written as

$$\gamma_t = \rho_{\text{time}}\gamma_{t-1} + \epsilon_t, \quad t = 2, \dots, T,$$

where  $\epsilon_2, \dots, \epsilon_T | \sigma_{\text{time}}^2 \stackrel{\text{iid}}{\sim} \mathcal{N}(0, \sigma_{\text{time}}^2)$ . Often the condition  $\gamma_1 | \rho_{\text{time}}, \sigma_{\text{time}}^2 \sim \mathcal{N}(0, \sigma_{\text{time}}^2 / (1 - \rho_{\text{time}}^2))$  is added to make the autoregressive process stationary.

The first-order random walk penalises the first-order differences through  $\gamma_2 - \gamma_1, \dots, \gamma_T - \gamma_{T-1} | \sigma_{\text{rw1}}^2 \stackrel{\text{iid}}{\sim} \mathcal{N}(0, \sigma_{\text{rw1}}^2)$ . The second-order random walk penalises the second-order differences through  $\gamma_3 - 2\gamma_2 + \gamma_1, \dots, \gamma_T - 2\gamma_{T-1} + \gamma_{T-2} | \sigma_{\text{rw2}}^2 \stackrel{\text{iid}}{\sim} \mathcal{N}(0, \sigma_{\text{rw2}}^2)$ . The first-order random walk has a rank deficiency of one and needs a sum-to-zero constraint to be identifiable together with an intercept. The second-order random walk has a rank deficiency of two, but usually only a sum-to-zero constraint is enforced. The remaining rank deficiency allows the second-order random walk to capture a linear trend.

#### A.4. The main spatial effect

The main spatial effect aims to describe spatial heterogeneity that is persistent in time. In an areal model, this is usually achieved by an areal model such as the Besag York and Mollié (BYM) model (Besag et al., 1991), whereas in a geostatistical model, this is usually achieved by Gaussian random field (GRF) with a Matérn covariance function.

The geostatistical model uses

$$\text{Space}(\mathbf{s}_{c,k}) = u(\mathbf{s}_{c,k}),$$

where  $u(\cdot)$  is a continuously indexed GRF parametrized through range,  $\rho_{\text{space}}$ , marginal variance,  $\sigma_{\text{space}}^2$ , and smoothness,  $\nu_{\text{space}}$ . A fast approach to perform inference with such models is the SPDE approach (Lindgren et al., 2011) with inference using the INLA approach (Rue et al., 2009).

A more untraditional approach is to consider  $A$  geographical areas and let the spatial effect be piece-wise constant on these areas. If we employ a BYM model for the values in the areas, we get

$$\text{Space}(\mathbf{s}_{c,k}) = \sigma_{\text{space}} \left( \phi_{\text{space}} v_{a[\mathbf{s}_{c,k}]} + \sqrt{1 - \phi_{\text{space}}^2} \delta_{a[\mathbf{s}_{c,k}]} \right),$$

where  $a[\mathbf{s}]$  denotes the area that contains the spatial location  $\mathbf{s}$ ,  $(v_1, \dots, v_A)$  follows a scaled Besag process (Sørbye and Rue, 2014), and  $\delta_1, \dots, \delta_A \stackrel{\text{iid}}{\sim} \mathcal{N}(0, 1)$ . If we enforce the constraint  $v_1 + \dots + v_A = 0$ , the parameter  $\sigma_{\text{space}}^2$  is approximately the marginal variance, and  $0 \leq \phi_{\text{space}}^2 \leq 1$  is the proportion of the marginal variance arising from the Besag component. Note that we are using the BYM model to construct a continuously indexed GRF.

### A.5. The spatio-temporal interaction

The spatio-temporal interaction aims to describe how spatial heterogeneity changes over time. In standard geostatistical models it is not common to include a separate main effect and spatio-temporal interaction. As such it is common to write

$$\text{Space}(\mathbf{s}_{c,k}) + \text{Space-Time}(\mathbf{s}_{c,k}, t) = u(\mathbf{s}_{c,k}, t),$$

where  $u(\cdot, \cdot)$  is a spatio-temporal GRF. In discrete time, it is easy to construct a separable spatio-temporal dependence structure by combining a spatial model with an autoregressive model. E.g.,

$$u(\mathbf{s}, t) = \psi_{\text{ST}} u(\mathbf{s}, t-1) + w_t(\mathbf{s}), \quad t = 2, \dots, T,$$

where  $w_2(\cdot), \dots, w_T(\cdot)$  are independent spatial Matérn GRFs with range  $\rho_{\text{ST}}$ , marginal variance  $\sigma_{\text{ST}}^2$ , and smoothness  $\nu_{\text{ST}}$ .

If the main spatial effect is defined through  $A$  geographical areas such as in Section A.4, one can include a spatio-temporal interaction in addition to the main spatial effect

$$\text{Space-Time}(\mathbf{s}_{c,k}, t) = b_{a[\mathbf{s}_{c,k}],t},$$

where  $(b_{1,1}, \dots, b_{A,1}, \dots, b_{A,T}) | \boldsymbol{\theta}_{\text{ST}} \sim \mathcal{N}_{AT}(0, \mathbf{Q}_{\text{ST}}(\boldsymbol{\theta}_{\text{ST}})^{-1})$ . The spatial structure is created through a separable dependence structure combining, e.g., an  $A \times A$  spatial Besag precision matrix  $\mathbf{Q}_{\text{Besag}}$  and  $T \times T$  first-order random walk precision matrix  $\mathbf{Q}_{\text{RW1}}$ . This would give  $\mathbf{Q}_{\text{ST}} = \mathbf{Q}_{\text{RW1}} \otimes \mathbf{Q}_{\text{Besag}}$ , where the dependence on parameters is suppressed in the notation for ease of reading. The temporal precision matrix can directly be changed to other temporal dependence structures such as a autoregressive processes. However, one should carefully consider the consequences of using temporal dependence structures that are more intrinsic than the first-order random walk. A second-order random walk has a rank deficiency of 2 and allows different linear trends in each area where there is no spatial smoothing of the trends across areas. To make the spatio-temporal interaction identifiable one can apply sum-to-zero constraints in time for every area, and sum-to-zero constraints in space for every time point.

### A.6. Priors

All variance and correlation parameters in the model components described in the previous sections must be assigned priors. A principled approach is to use penalised complexity (PC) priors (Simpson et al., 2017). Simpson et al. (2017) provide details for variance parameters, (Sørbye and Rue, 2017) provide details for autoregressive processes, Riebler et al. (2016) provide details for BYM models, and Fuglstad et al. (2019) provide details for Matérn GRFs. Such priors have successfully been applied using **SUMMER** (Li et al., 2021) across many countries (Li et al., 2019; UN IGME, 2021; Wu et al., 2021). This illustrates that with sensible hyperparameters, this class of priors work well across diverse countries for spatio-temporal estimation, but results should be always be investigated for anomalous behaviour. Specific choices of priors and hyperparameters are given in the case studies in Sections B.5 and C.3.

**Table B.1.** Number of EAs in urban and rural strata for each admin1 area. In total, 276058 urban EAs and 388941 rural EAs. The numbers are from National Population Commission - NPC and ICF (2019).

Admin1	Urban	Rural	Admin1	Urban	Rural
Abia	2106	9463	Kano	16957	19402
Adamawa	2820	9988	Katsina	6874	26442
Akwa Ibom	908	16205	Kebbi	14020	2621
Anambra	18409	3498	Kogi	5492	10354
Bauchi	2761	17124	Kwara	11715	4556
Bayelsa	2628	6379	Lagos	25424	0
Benue	2006	20850	Nasarawa	2008	7211
Borno	7798	16288	Niger	5126	18319
Cross River	1410	14912	Ogun	7085	7408
Delta	9008	9201	Ondo	8588	10667
Ebonyi	11911	1977	Osun	19810	6097
Edo	7964	4829	Oyo	22405	8701
Ekiti	9438	2123	Plateau	3949	11930
Enugu	9774	4223	Rivers	12480	12381
FCT Abuja	2452	1138	Sokoto	2548	10231
Gombe	1955	7539	Taraba	1657	8943
Imo	10006	9567	Yobe	3053	11870
Jigawa	2293	18900	Zamfara	3090	13942
Kaduna	9529	12263			

## B. Case study: Nigeria

In this section, we denote cluster index by  $c = 1, \dots, M$ , where  $M = 1324$  is the number of clusters, and we denote the location of cluster  $c$  by  $s_c$ . The number of areas in the administrative level is  $A$  and the individual areas are indexed by  $a = 1, \dots, A$ . Throughout the section, we assume that the cluster index run over all possible values unless otherwise specified. Observations consist of number of children  $n_c$

### B.1. Details on enumeration areas

The 664999 EAs are distributed to the 37 states as shown in Table B.1.

### B.2. Covariate rasters

We use two covariates:

- **Poverty:** Worldpop 2010 estimates of proportion of people per grid square living in poverty, as defined by \$2 a day threshold. URL: <https://www.worldpop.org/geodata/summary?id=1267>.
- **Access:** Malaria Mapping Project 2015 Map of Travel Time to Cities. URL: <https://malariaatlas.org/explorer/>. (Weiss et al., 2018).

Both covariates are converted to matching  $1 \text{ km} \times 1 \text{ km}$  raster that covers Nigeria. The values are shown in Figure B.1.

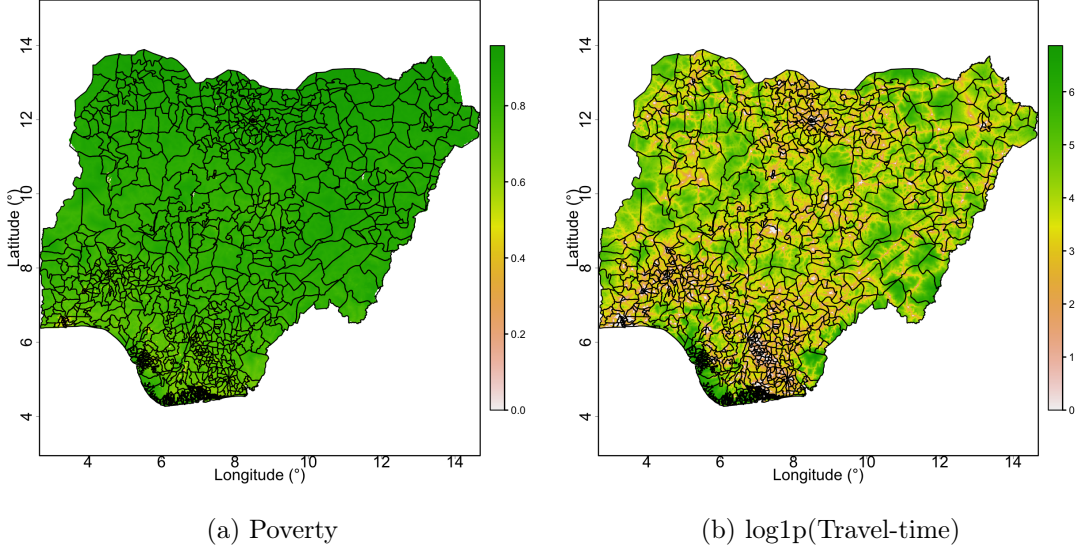


**Figure B.1.** The two covariate rasters: proportion of people per  $1 \text{ km} \times 1 \text{ km}$  grid cell living in poverty (as defined by \$2 per day), and the  $\log_{1p}(x) = \log(1 + x)$  transformation of travel-time to nearest city.

### B.3. Urban/rural classification

Using the procedure described in the main paper, we constructed a  $100 \text{ m} \times 100 \text{ m}$  raster with values 1 (urban) and 0 (rural). The raster is a refinement of the covariate rasters in Section B.2 such that each  $1 \text{ km} \times 1 \text{ km}$  grid cell is divided into 100 smaller grid cells. The resulting raster is shown in Figure B.2.

### B.4. Triangulation used for SPDE approach

We implement an approximate Matérn GRF using the SPDE approach (Lindgren et al., 2011) with the mesh shown in Figure B.3. The mesh has 6888 vertexes.

### B.5. Model details

Let  $p_a$  denote the prevalence in area  $a$ . We denote the number of observed children and the number of children with outcome 1 by  $n_c$  and  $y_c$ , respectively. We consider seven approaches:

1. **NoSpace:** Baseline model used when comparing scores. This model has no spatial variation,

$$Y_c | n_c, R_c \sim \text{Binomial}(n_c, R_c), \quad \text{independently for } c = 1, \dots, M,$$

$$\text{logit}(R_c) = \mu + \mathbf{z}_c^T \boldsymbol{\beta} + \epsilon_c,$$

where  $\mu$  is the intercept,  $z_c$  is 1 (urban) or 0 (rural), and  $\boldsymbol{\beta}$  is the effect of urban, and  $\epsilon_1, \dots, \epsilon_M | \sigma_N^2 \stackrel{\text{iid}}{\sim} \mathcal{N}(0, \sigma_N^2)$ .

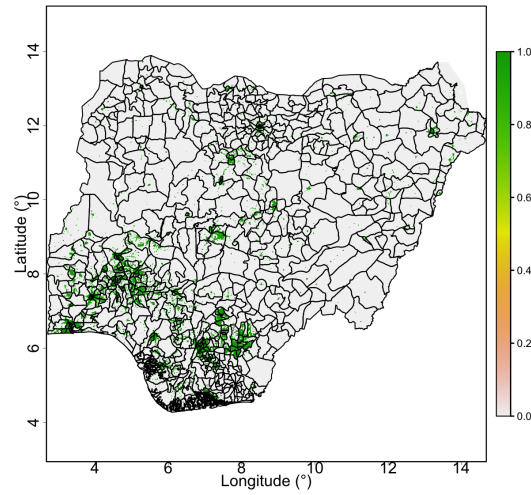


**Figure B.2.** Map of estimated urban and rural locations for NDHS2018 sampling frame. Green is urban and grey is rural.

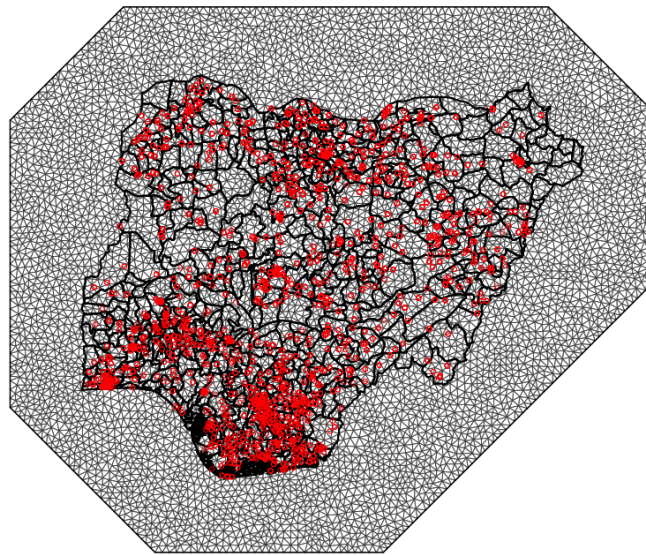


**Figure B.3.** Mesh used for the SPDE approach. There are 6888 vertexes and the red circles show the locations of the observed clusters.

We let  $\mu$  have a flat prior,  $\beta \sim \mathcal{N}(0, 1000)$ , and  $\sigma_N^2$  has the PC prior (Simpson et al., 2017) with hyperparameter set according to  $P(\sigma_N > 1) = 0.05$ .

2. **Dir-A1:** Direct estimates that account for the complex survey design are computed using the R-package `survey` (Lumley, 2018). This provides estimates  $\widehat{\text{logit}(p_a)}$  with associated variance estimates  $\hat{V}_a$ . We assume that the sample distributions are given by  $\widehat{\text{logit}(p_a)} \sim \mathcal{N}(\text{logit}(p_a), \hat{V}_a)$ . There is independence between different areas as observations are not shared between areas.
3. **SDir-A1:** This model concerns admin1 and there are  $A = 37$  admin1 areas. We first compute  $\text{logit}(p_a)$  and  $\hat{V}_a$  using Dir-A1. Then employ the spatial smoothing model

$$\begin{aligned} \widehat{\text{logit}(p_a)}|p_a &\sim \mathcal{N}(\text{logit}(p_a), \hat{V}_a), \quad \text{independently for } a = 1, \dots, A, \\ \text{logit}(p_a) &= \mu + \sigma_{\text{space}} \left( \phi_{\text{space}} v_a + \sqrt{1 - \phi_{\text{space}}^2} \delta_a \right) + \epsilon_a, \end{aligned}$$

where  $\mu$  is the intercept,  $(v_1, \dots, v_{37})$  is a scaled Besag model (Sørbye and Rue, 2014) on the admin1 graph,  $\delta_1, \dots, \delta_{37} \stackrel{\text{iid}}{\sim} \mathcal{N}(0, 1)$ , and  $\epsilon_1, \dots, \epsilon_A | \sigma_N^2 \stackrel{\text{iid}}{\sim} \mathcal{N}(0, \sigma_N^2)$ .

We let  $\mu$  have a flat prior,  $\phi_{\text{space}}$  and  $\sigma_{\text{space}}$  have the PC prior from Riebler et al. (2016) with hyperparameters set according to  $P(\sigma_{\text{space}} > 1) = 0.05$  and  $P(\phi_{\text{space}} > 0.5) = 0.50$ , and  $\sigma_N^2$  has the PC prior (Simpson et al., 2017) with hyperparameter set according to  $P(\sigma_N > 1) = 0.05$ .

4. **Spat-A1:** This model concerns admin1 and there are  $A = 37$  admin1 areas. We model the data by

$$\begin{aligned} Y_c | n_c, R_c &\sim \text{Binomial}(n_c, R_c), \quad \text{independently for } c = 1, \dots, M, \\ \text{logit}(R_c) &= \mu + z_c \beta + \sigma_{\text{space}} \left( \phi_{\text{space}} v_{a[\mathbf{s}_c]} + \sqrt{1 - \phi_{\text{space}}^2} \delta_{a[\mathbf{s}_c]} \right) + \epsilon_c, \end{aligned}$$

where  $\mu$  is the intercept,  $z_c$  is 1 (urban) or 0 (rural), and  $\beta$  is the effect of urban,  $(v_1, \dots, v_{37})$  is a scaled Besag model (Sørbye and Rue, 2014) on the admin1 graph,  $\delta_1, \dots, \delta_{37} \stackrel{\text{iid}}{\sim} \mathcal{N}(0, 1)$ , and  $\epsilon_1, \dots, \epsilon_M | \sigma_N^2 \stackrel{\text{iid}}{\sim} \mathcal{N}(0, \sigma_N^2)$ .

We let  $\mu$  have a flat prior,  $\beta \sim \mathcal{N}(0, 1000)$ ,  $\phi_{\text{space}}$  and  $\sigma_{\text{space}}$  have the PC prior from Riebler et al. (2016) with hyperparameters set according to  $P(\sigma_{\text{space}} > 1) = 0.05$  and  $P(\phi_{\text{space}} > 0.5) = 0.50$ , and  $\sigma_N^2$  has the PC prior (Simpson et al., 2017) with hyperparameter set according to  $P(\sigma_N > 1) = 0.05$ .

5. **Spat-A2:** This model concerns admin2 and there are  $A = 774$  admin2 areas. We model the data by

$$\begin{aligned} Y_c | n_c, R_c &\sim \text{Binomial}(n_c, R_c), \quad \text{independently for } c = 1, \dots, M, \\ \text{logit}(p_c) &= \mu + z_c \beta + \sigma_{\text{space}} \left( \phi_{\text{space}} v_{a[\mathbf{s}_c]} + \sqrt{1 - \phi_{\text{space}}^2} \delta_{a[\mathbf{s}_c]} \right) + \epsilon_c, \end{aligned}$$

where  $\mu$  is the intercept,  $z_c$  is 1 (urban) or 0 (rural), and  $\beta$  is the effect of urban,  $(v_1, \dots, v_{774})$  is a scaled Besag model (Sørbye and Rue, 2014) on the admin2 graph,  $\delta_1, \dots, \delta_{774} \stackrel{\text{iid}}{\sim} \mathcal{N}(0, 1)$ , and  $\epsilon_1, \dots, \epsilon_M | \sigma_N^2 \stackrel{\text{iid}}{\sim} \mathcal{N}(0, \sigma_N^2)$ .

We let  $\mu$  have a flat prior,  $\beta \sim \mathcal{N}(0, 1000)$ ,  $\phi_{\text{space}}$  and  $\sigma_{\text{space}}$  have the PC prior from Riebler et al. (2016) with hyperparameters set according to  $P(\sigma_{\text{space}} > 1) = 0.05$  and  $P(\phi_{\text{space}} > 0.5) = 0.50$ , and  $\sigma_{\text{N}}^2$  has the PC prior (Simpson et al., 2017) with hyperparameter set according to  $P(\sigma_{\text{N}} > 1) = 0.05$ .

6. **Spat-C:** This model allows the spatial effect to vary continuously in space. We model the data by

$$Y_c | n_c, R_c \sim \text{Binomial}(n_c, R_c), \quad \text{independently for } c = 1, \dots, M,$$

$$\text{logit}(R_c) = \mu + z_c \beta + u(\mathbf{s}_c) + \epsilon_c,$$

where  $\mu$  is the intercept,  $z_c$  is 1 (urban) or 0 (rural), and  $\beta$  is the effect of urban,  $u(\cdot)$  is an approximate Matérn GRF with range  $\rho$ , marginal variance  $\sigma^2$  and fixed smoothness  $\nu = 1$ , and  $\epsilon_1, \dots, \epsilon_M | \sigma_{\text{N}}^2 \stackrel{\text{iid}}{\sim} \mathcal{N}(0, \sigma_{\text{N}}^2)$ .

We let  $\mu$  have a flat prior,  $\beta \sim \mathcal{N}(0, 1000)$ ,  $\rho$  and  $\sigma^2$  have the PC prior from Fuglstad et al. (2019) with hyperparameters set according to  $P(\rho > 3) = 0.50$  and  $P(\phi_{\text{space}} > 0.5) = 0.50$ , and  $\sigma_{\text{N}}^2$  has the PC prior (Simpson et al., 2017) with hyperparameter set according to  $P(\sigma_{\text{N}} > 1) = 0.05$ .

7. **Spat-Cov:** This model allows the spatial effect to vary continuously in space. We model the data by

$$Y_c | n_c, R_c \sim \text{Binomial}(n_c, R_c), \quad \text{independently for } c = 1, \dots, M,$$

$$\text{logit}(R_c) = \mu + \mathbf{z}_c^T \boldsymbol{\beta} + u(\mathbf{s}_c) + \epsilon_c,$$

where  $\mu$  is the intercept,  $\mathbf{z}_c$  is vector of length 3 with the three covariates urban/rural (1/0), poverty and access, and  $\boldsymbol{\beta}$  is a vector of length 3 with the effects of the covariates,  $u(\cdot)$  is an approximate Matérn GRF with range  $\rho$ , marginal variance  $\sigma^2$  and fixed smoothness  $\nu = 1$ , and  $\epsilon_1, \dots, \epsilon_M | \sigma_{\text{N}}^2 \stackrel{\text{iid}}{\sim} \mathcal{N}(0, \sigma_{\text{N}}^2)$ .

We let  $\mu$  have a flat prior,  $\beta_1, \beta_2, \beta_3 \stackrel{\text{iid}}{\sim} \mathcal{N}(0, 1000)$ ,  $\rho$  and  $\sigma^2$  have the PC prior from Fuglstad et al. (2019) with hyperparameters set according to  $P(\rho > 3) = 0.50$  and  $P(\phi_{\text{space}} > 0.5) = 0.50$ , and  $\sigma_{\text{N}}^2$  has the PC prior (Simpson et al., 2017) with hyperparameter set according to  $P(\sigma_{\text{N}} > 1) = 0.05$ .

### B.6. Comparison of point estimates

The admin1 point estimates for all six models are shown in Figure B.4, and the point estimates and associated uncertainties are shown in Figure B.5 for Spat-A2, Spat-C, and Spat-Cov.

### B.7. Computing scores

Let  $p_a$  denote the prevalence in area  $a$ . We denote the number of observed children and the number of children with outcome 1 by  $n_c$  and  $y_c$ , respectively. We consider two scoring strategies: scoring areal estimates and scoring cluster predictions.

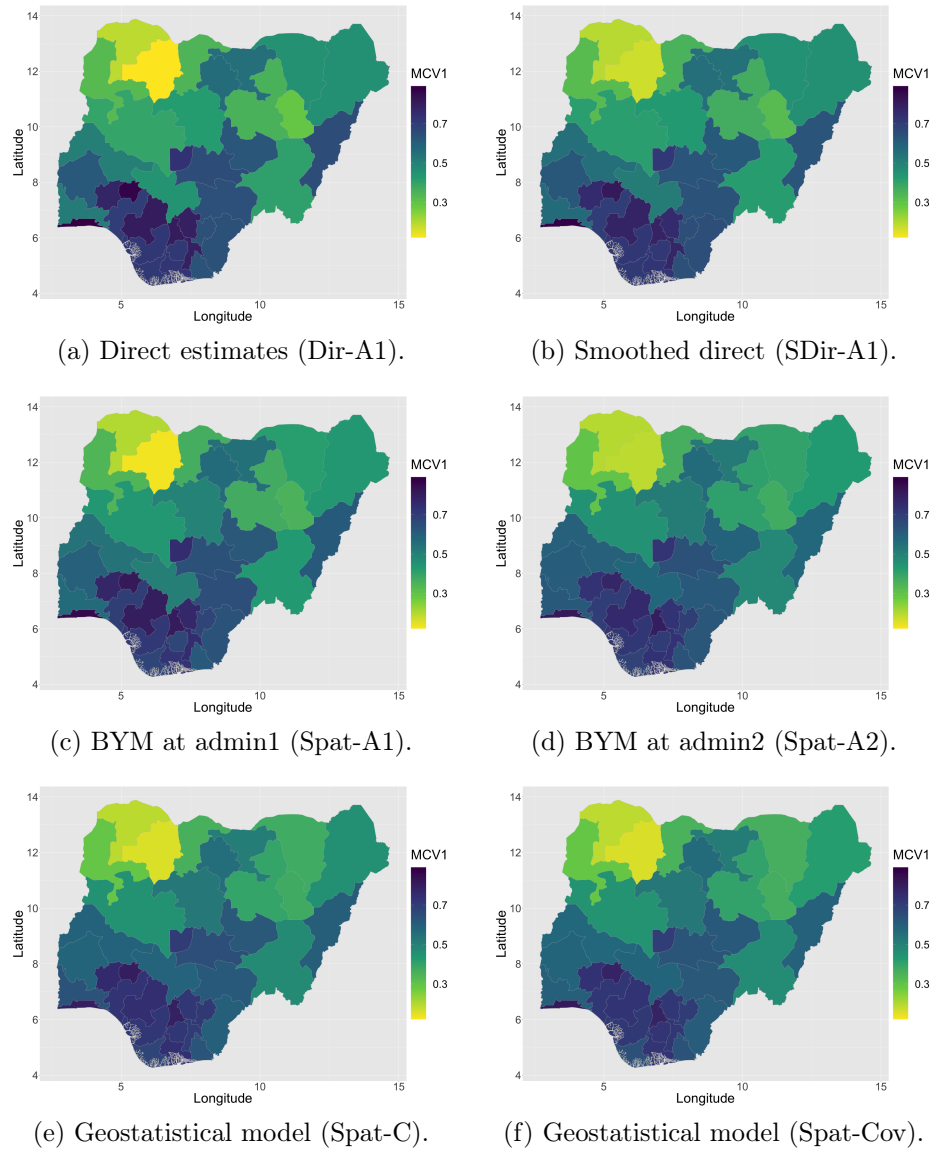


**Figure B.4.** Comparison of aggregate estimates of vaccination coverage for admin1 areas. The maps show posterior medians and models are specified in captions of the subfigures.



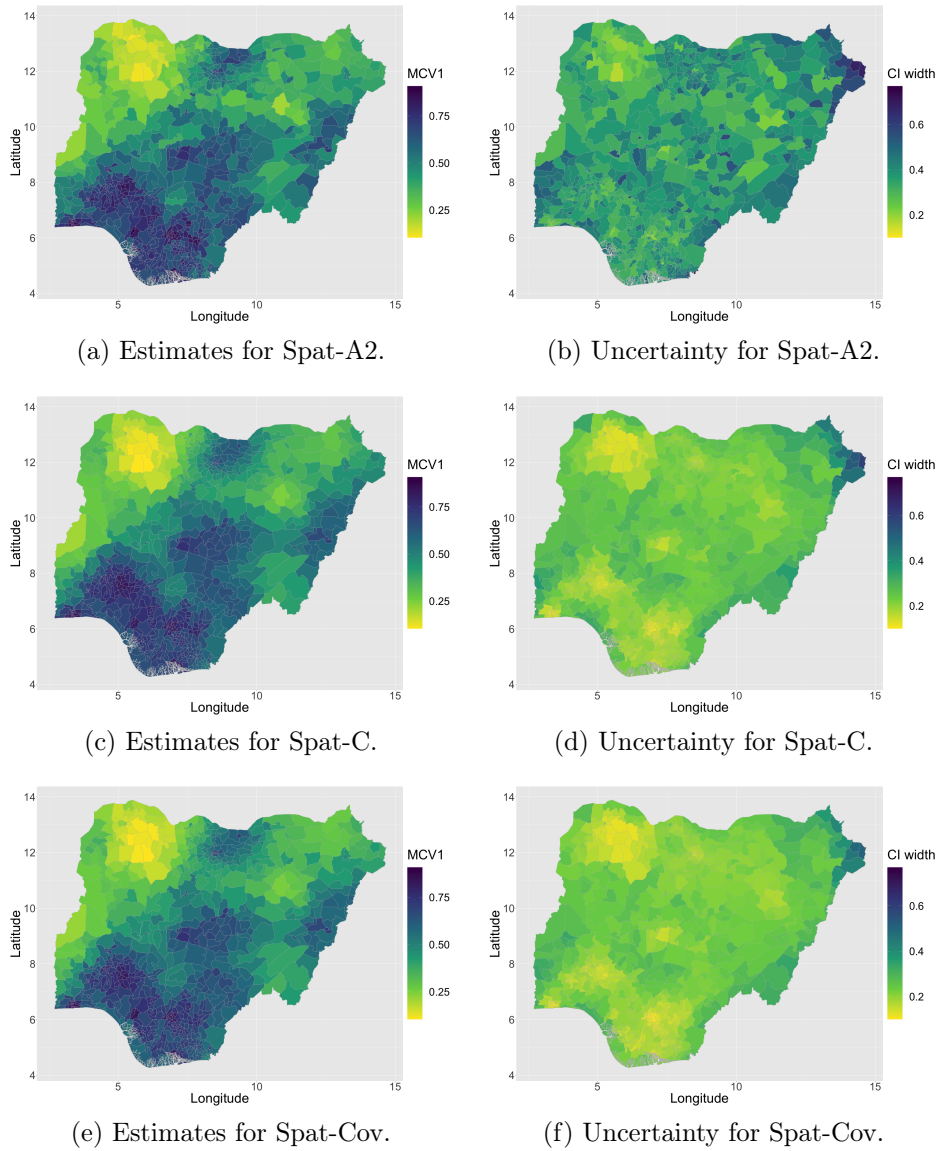


**Figure B.5.** Admin2 estimates of vaccination coverages. The uncertainty is quantified by the length of the 95% credible interval.

*B.7.1. Scoring admin1 estimates*

We follow Section B.5, and assume that the direct estimators have the sampling distribution  $\widehat{\text{logit}}(p_a) \sim \mathcal{N}(\text{logit}(p_a), \hat{V}_a)$ , where  $\hat{V}_a$  is the direct estimate of the variance. If we hold out area  $b$  when estimating the model, the posterior  $\pi(p_b | \text{Data excluding area } b)$  is independent of  $\widehat{\text{logit}}(p_b)$  because they are based on independent data.

Let  $h_b$  be the observed value of  $\widehat{\text{logit}}(p_b)$ , then we can view  $h_b$  as a noisy observation of the true value  $\text{logit}(p_b)$ . The key observation is that if we combine the independent sampling distribution of the direct estimator with the model-based posterior for the true value  $\text{logit}(p_b)$ , we find a predictive distribution  $\pi(h_b | \text{Data excluding area } b)$ . This allows us to directly score performance for estimation of areal prevalences. The discriminatory power of this approach depends on the size of  $\hat{V}_b$  versus the sharpness of the model-based posteriors.

Use  $H_b$  to denote the stochastic variable, and  $h_b$  to be the observed value. We compute two scores:

- **MSE:**

$$\text{MSE} = \frac{1}{37} \sum_{b=1}^{37} (h_b - \text{median}[H_b | \text{"Data excluding area } b"])^2.$$

- **LogScore:**

$$\text{LogScore} = \frac{1}{37} \sum_{b=1}^{37} -\log(\pi(H_b = h_b | \text{"Data excluding area } b")).$$

The negative sign in the log-score ensures that lower is better for both MSE and LogScore.

*B.7.2. Scoring cluster predictions*

Cluster predictions are scored in a standard way through 10-fold cross validation. The clusters are randomly divided into 10 folds, each fold is held out in turn, and the response in the hold-out clusters is predicted. Scores are computed by comparing the observed proportion of vaccinated children with predicted proportion of vaccinated children. We compute both MSE and the log-score averaged over all clusters.

*B.8. Diagnostics: sharing effect of urban/rural*

We use the assumption that we can use the same effect of urban versus rural in all 37 admin1 areas. We investigate this assumption by modifying NoSpace to use 37 separate coefficients of urban versus rural  $\beta_a$ ,  $a = 1, \dots, 37$ . Figure B.6 demonstrates that this assumption is not unreasonable given the amount of information available in the data. The large mismatch for  $a = 25$  is because everyone was vaccinated in the rural part of area  $a = 25$ , and should be ignored.

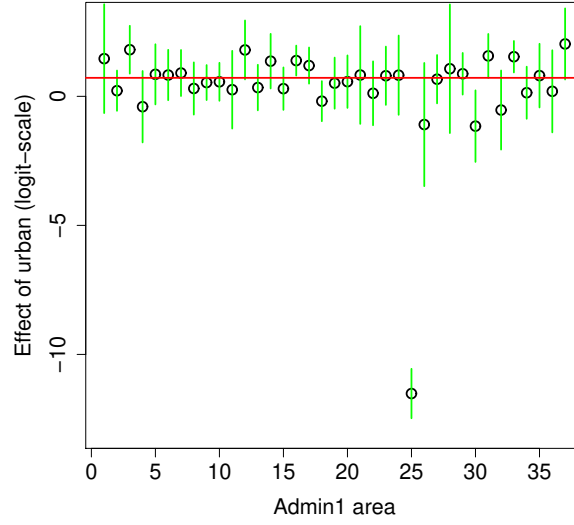


**Figure B.6.** Estimated effects  $\beta_a$  of urban versus rural for admin1 areas  $a = 1, \dots, 37$ . The green lines show 95% credible intervals. Note that estimation breaks down for area 25 to observing everyone vaccinated in the rural part of the area. The red line shows the corresponding estimate when  $\beta_1 = \dots = \beta_{37}$ .

## C. Case study: Malawi

### C.1. Urban/rural fractions

The master sampling frame from the 2008 census is not publicly available. But the urban and rural population in the 28 districts is reported in the 2008 Malawi Census (Malawi National Statistical Office, 2008). We note that while the final report for MDHS2015 provide the proportion of urban and rural households in each of the 28 districts at the time of survey, these do not correspond to the proportions of urban and rural population as average size of households may differ for urban and rural households, and in different districts. The most reliable information about the urban/rural population is only available for the year of 2008.

We obtained yearly raster maps from WorldPop providing high-resolution maps of population density in Malawi for 2000–2019. To obtain urban/rural fractions, we use a similar procedure to that used for vaccination coverage in Nigeria. We use the population density map for 2008 to select a threshold such that the proportion of the urban population in each region matches that from the 2008 Malawi Census. This allows us to create the urban/rural partition for each district in 2008, as shown in Figure C.1. We then use the fixed partition to obtain the proportion of the “urban population” for the remainder of the years. The estimated proportion of population living in the urban partition remains relatively constant over the period.

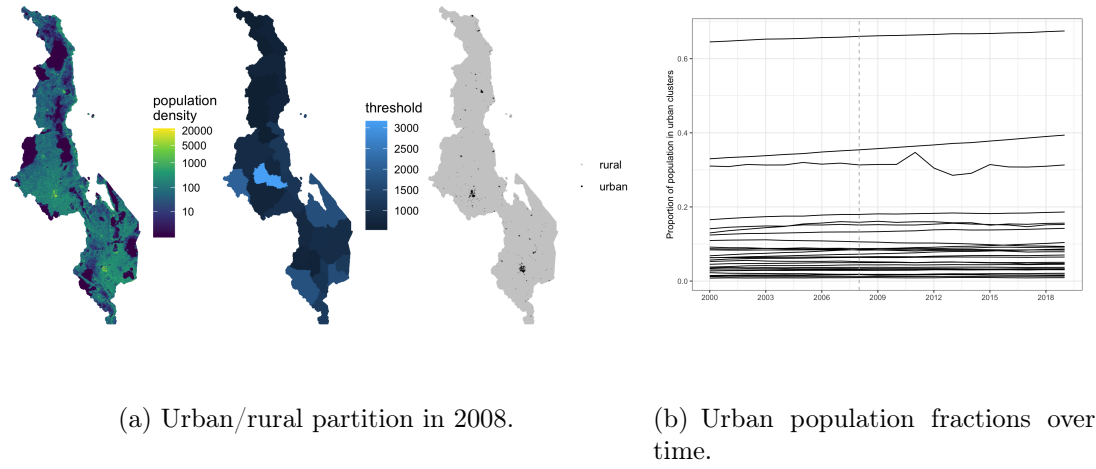
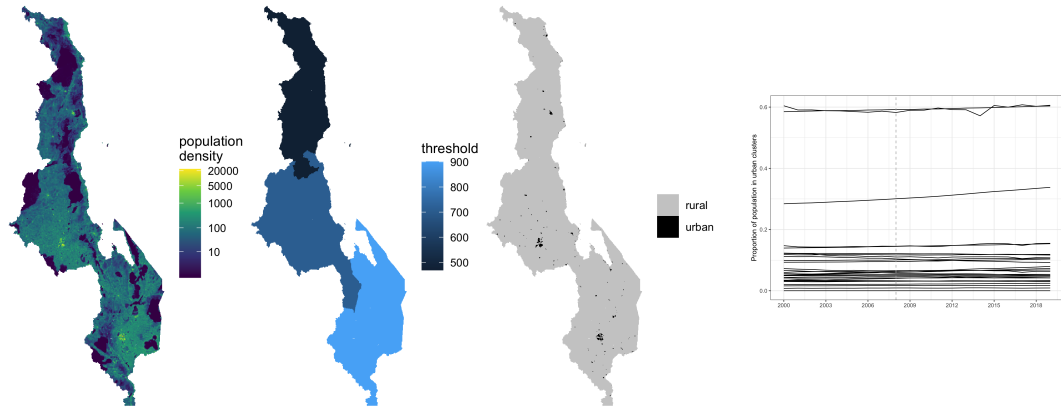


**Figure C.1.** Left: Population density in 1km by 1km pixels, estimated threshold of urban partition in the 28 districts, and the estimated urban partition, based on the 2008 Malawi census and WorldPop population map. Right: Estimated fraction of population in the urban partition defined by the 2008 census in each of the 28 districts from 2000 to 2019.

### C.2. Comparing different urban/rural partitions

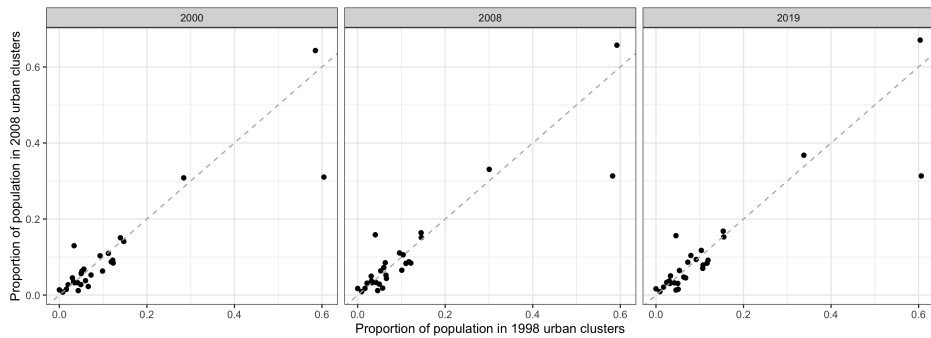
We consider adding the MDHS 2004 survey into our model in this section. The MDHS 2004 survey is based on the enumeration areas in the 1998 census, thus with a different urban/rural definition compared to later surveys. To compute the implied urban/rural partition, we first threshold the population density map of Malawi in 2000 to match the reported urban/rural population fractions in the 1998 census. We use the 2000 population density map because it is the earliest available population information provided by Worldpop. For the 1998 census, population densities by urban/rural strata is only available at the three larger regions shown in Figure 2(a). We performed the same thresholding procedure for the three regions as described in the manuscript and obtained the partition and population fraction by strata over time in Figure C.2. Figure 2(c) shows a comparison of estimated population fraction in urban partitions defined by the two censuses.

The different partitions also leads to dramatically different levels and trends of NMR by stratum. To illustrate this, we combine the MDHS 2004 data in the analysis in the main paper and treat the two sets of stratification as four fixed effects. This leads to four set of stratum-specific NMR. Figure C.3 shows the national estimates of stratum-specific NMR for the four strata. The NMR for urban partitions defined by the two censuses show a considerable differences, which is not surprising as the urban regions likely changed more dramatically between 1998 and 2008.



(a) Urban/rural partition in 2000.

(b) Urban population fractions over time.



(c) Comparison of the urban population fractions defined by different censuses.

**Figure C.2.** Panel (a): Population density in 1km by 1km pixels, estimated threshold of urban partition in the 28 district, and the estimated urban partition, based on the 1998 Malawi census and 2000 WorldPop population map. Panel (b): Estimated fraction of population in the urban partition defined by the 1998 census in each of the 28 districts from 2000 to 2019. Panel (c): Comparison of the fraction of population in urban partitions defined by the 1998 census and the 2008 census in selected years.

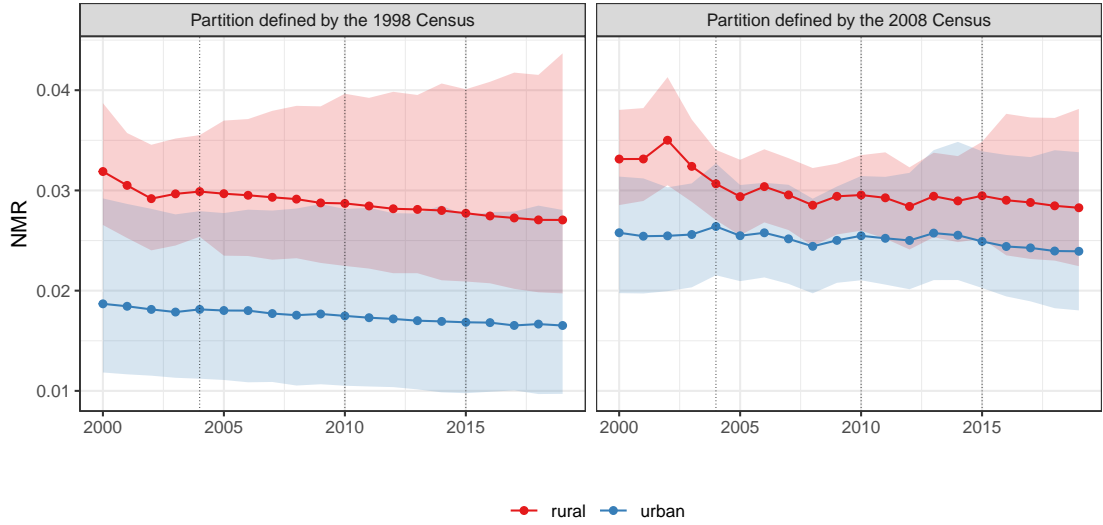


**Figure C.3.** Comparing stratum-specific national estimates of NMR for the stratification defined in two different sampling frames.

### C.3. Model details

For the space-time smoothing of NMR presented in the main paper, we model the main temporal term with AR(1) processes with PC prior on the variance so that  $P(\sigma_{RW2} > 0.5) = 0.01$ , and a linear trend modeled with fixed effect and prior  $N(0, 1000)$ . We model the space-time interaction term with a separable combination of an AR(1) process in time and a Besag model in space, with hyperprior  $P(\sigma_{Int} > 0.5) = 0.01$  for the variance and  $P(\omega > 0.7) = 0.9$  for the autocorrelation correlation coefficient  $\omega$ . We also allow area-specific deviations from the main temporal trends by including area-specific random slopes. We scale the time index to be from  $-0.5$  to  $0.5$  so that the random slope has the interpretation of the total deviation from the main trend during the entire period. We let the random slopes  $\{b_i\}_{i=1,\dots,28}$  follow a Gaussian distribution with PC priors on the variance so that  $P(b_i > 1) = 0.01$ .

### C.4. Additional results for NMR estimation in Malawi

Figure C.4 shows the time-varying odds ratios associated with clusters in the urban partition. The association is strong before 2004 and becomes closer to zero in the last twenty years. Figure C.5 shows the district-stratum-specific estimates of NMR in the analysis in the main manuscript. Figure C.6 compares the direct estimates, smoothed direct estimation, and the estimates from the Beta-Binomial model. Figure C.7 to C.9 shows the posterior distribution of the rankings of the 28 regions in 2000, 2009, and 2019 respectively, with rank = 1 corresponding to lowest NMR and rank = 28 corresponding to the highest NMR.

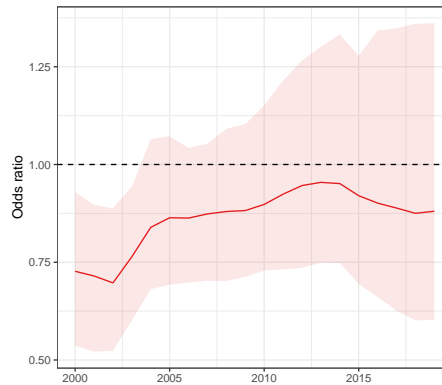


**Figure C.4.** The posterior median of the odds ratio associated with being urban and the 95% credible interval.

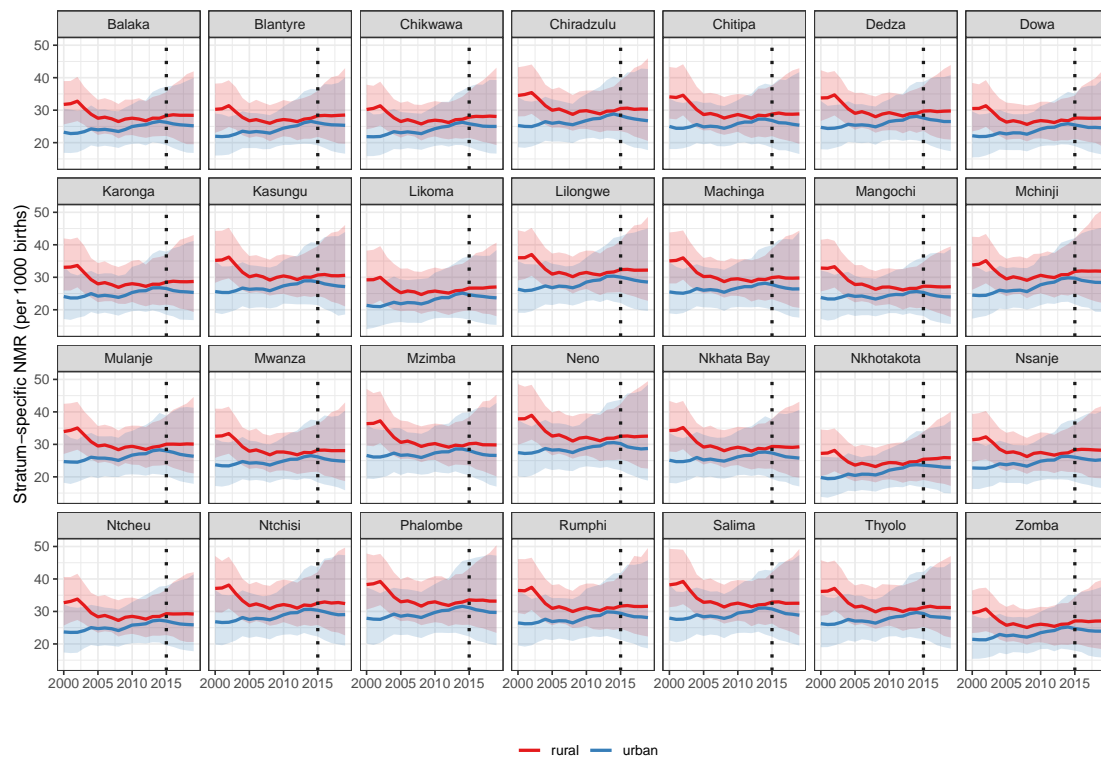


**Figure C.5.** Comparing estimates of urban and rural NMR in the 28 districts of Malawi.



**Figure C.6.** Comparing estimates the direct estimates, smoothed direct estimates, and the model-based estimates of NMR in the 28 districts of Malawi.



Ranking of districts in 2000

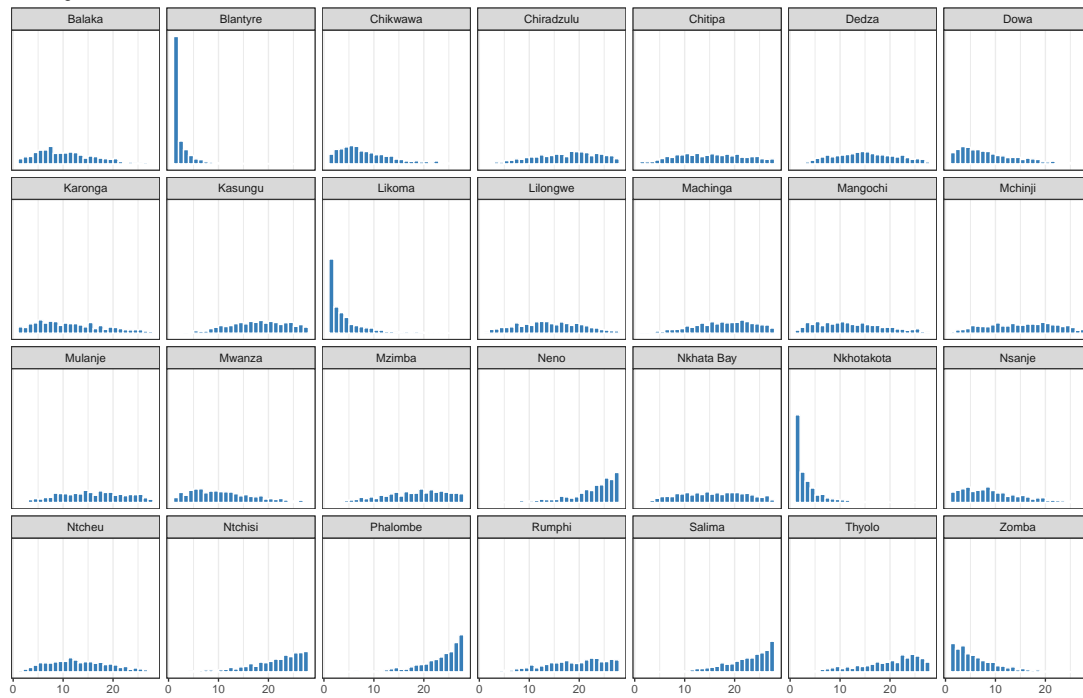


**Figure C.7.** Posterior distribution of the rankings of the 28 district based on estimated NMR in 2000. Lower values correspond to lower NMR estimates. Rank = 1 corresponds to lowest NMR and rank = 28 corresponds to the highest NMR.

Ranking of districts in 2009

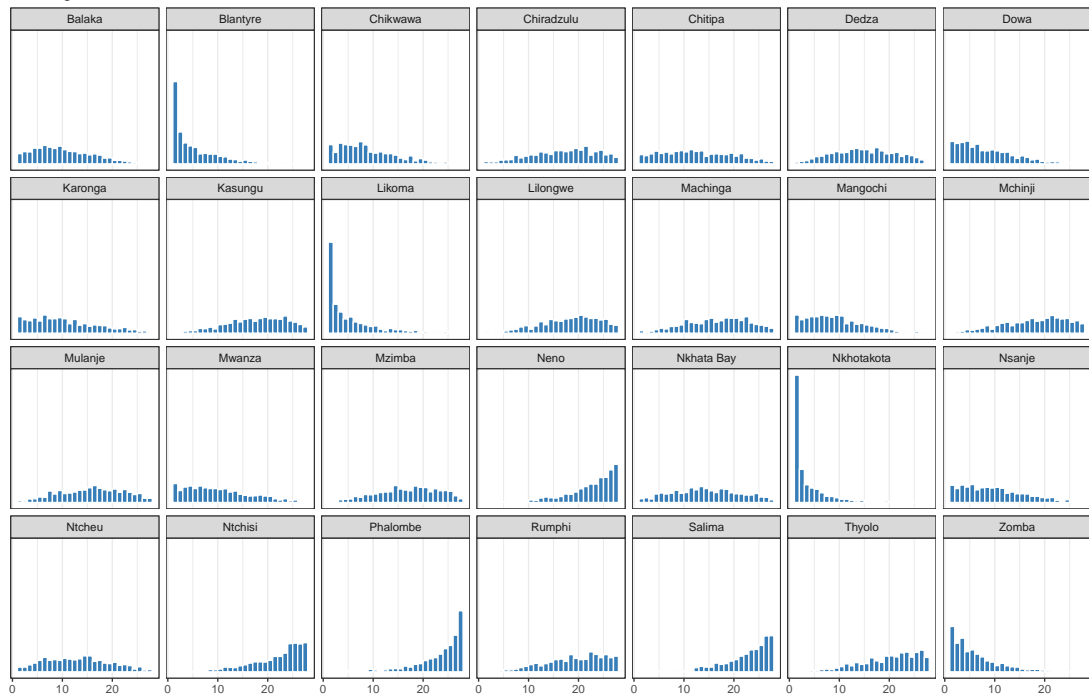


**Figure C.8.** Posterior distribution of the rankings of the 28 district based on estimated NMR in 2009. Lower values correspond to lower NMR estimates. Rank = 1 corresponds to lowest NMR and rank = 28 corresponds to the highest NMR.

Ranking of districts in 2019

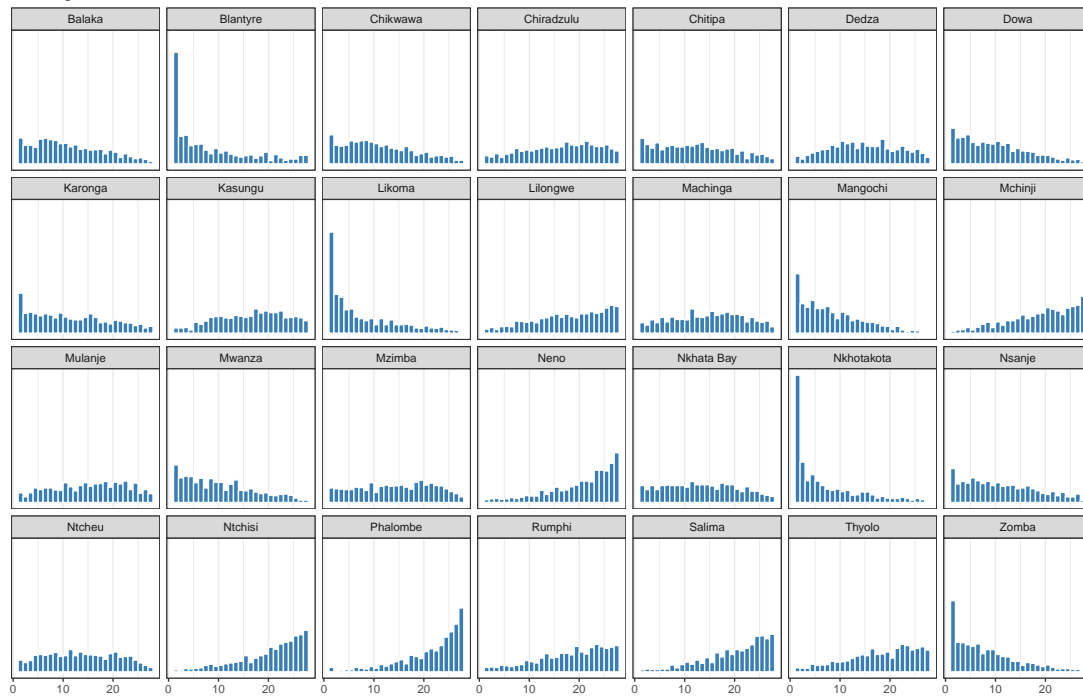


**Figure C.9.** Posterior distribution of the rankings of the 28 district based on estimated NMR in 2019. Lower values correspond to lower NMR estimates. Rank = 1 corresponds to lowest NMR and rank = 28 corresponds to the highest NMR.